UNIVERSITY OF CALIFORNIA

Radiation Laboratory

BERKELEY, CALIFORNIA

DISCLAIMER

UCRL-2325
Unclassified-Chemistry Distribution

UNIVERSITY OF CALIFORNIA

Radiation Laboratory

Contract No. W-7405-eng-48

ORBITAL ELECTRON CAPTURE IN THE HEAVIEST ELEMENTS

Richard William Hoff

(Thesis)

September, 1953

Berkeley, California

TABLE OF CONTENTS

ORBITAL ELECTRON CAPTURE IN THE HEAVIEST ELEMENTS

Richard W. Hoff
Radiation Laboratory and Department of Chemistry
University of California, Berkeley, California

September 1953

ABSTRACT

Certain isotopes in the region of the heaviest elements have been produced by cyclotron and pile bombardment techniques, and their nuclear decay properties have been investigated. The orbital electron capture decay of At^{210}, At^{211}, Np^{234}, Np^{235}, Pu^{234}, Pu^{237}, and Am^{242m} has been studied and decay schemes have been proposed. In addition, the alpha spectra of Po^{211}, At^{210}, and At^{211} have been observed.

The decay energy, as determined from closed decay cycles and the proposed decay scheme, and the observed half-life for the electron capture of the experimentally studied nuclides have been correlated with beta decay theory for allowed and forbidden transitions. Certain other known electron capture nuclides in the heaviest elements where decay energies may also be calculated from closed decay cycles have been treated in a similar manner. The observed K/L electron capture ratios have shown agreement with theoretically predicted values in most cases. A logarithmic plot of the electron capture partial half-life versus neutrino energy has been made for both the allowed and first forbidden species. Approximate agreement has been shown between the observed slope and the slope predicted by electron capture theory for a straight line drawn through the points for each type of transition.

ORBITAL ELECTRON CAPTURE IN THE HEAVIEST ELEMENTS

Richard W. Hoff
Radiation Laboratory and Department of Chemistry
University of California, Berkeley, California

September 1953

I. INTRODUCTION

Orbital electron capture as a means of radioactive decay may be classified under the more general term, beta decay. Beta decay of a nuclide can occur when the parent nucleus is unstable toward, i.e., heavier than, a neighboring isobar with the resultant transformation of a neutron within the nucleus into a proton or vice versa. The conversion of a neutron within the nucleus to a proton results in the creation and emission of a negative electron and an antineutrino from the nucleus. The opposite process, transformation of a proton into a neutron, results in the creation and emission of a positive electron and a neutrino from the nucleus. Conversely, it is possible for an orbital electron to be captured by a nucleus, a proton transformed to a neutron, and a neutrino, supposedly identical in properties to an antineutrino, emitted. A fourth possible means of beta decay is the capture of a positive electron by the nucleus. However, since positive electrons are not readily available to the nucleus, this method of decay is not observed.

"Beta minus" decay is displayed by nuclei with neutron to proton ratios greater than those for beta stable nuclei of a given element, while positron and orbital electron capture decay are demonstrated by nuclei with neutron to proton ratios smaller than

those of the beta stable nuclei of an element. Positron decay is limited energetically to those transitions where more than 1.02 Mev energy is available between atomic masses required for the creation of two electrons. Electron capture decay requires only enough energy to overcome the binding energy of the electron in the particular shell which the orbital electron originally occupied.

Electron capture decay is observed throughout the periodic table, but predominates relative to positron decay in the region of the heaviest elements. As the charge on the nucleus increases, electron capture becomes more and more probable because the density of electrons near the nucleus increases and the increased nuclear charge inhibits positron emission. Hence, for the elements above mercury ($Z > 80$) positron emission has not been detected and electron capture becomes the only means of beta decay observed for the neutron deficient isotopes of a given element. At the same time, the elements in the heavy region ($Z \geq 79$) are unstable toward decay by alpha emission. Thus, in many cases branching decay is observed and decay by electron capture is seen to compete favorably with alpha decay for the neutron deficient isotopes of a given element.

When orbital electron capture occurs, the decay energy in excess of the binding energy of the electron in its shell is dissipated as kinetic energy of the emitted neutrino and the recoil nucleus. Since the neutrino has a very small rest mass, a large fraction of this energy is carried off by the neutrino. The vacancy

in the electron shell created by the capture of the electron is filled by electrons of outer shells with the resultant emission of x-rays. The electron capture process may leave the daughter nucleus in an excited state and one or more gamma rays may be emitted in decay to the ground state. Thus, although the presence of electron capture may be detected by the observation of x-rays of the daughter element, no simple means is available for the determination of the decay energy since the neutrino, a neutral particle, has only been observed indirectly through the recoil of the daughter nucleus. A neutrino would not be expected to interact very strongly with any known particle.

A refinement of alpha decay systematics[1] has enabled the accurate prediction of alpha decay energies for most of the heaviest elements. Furthermore, the past few years have witnessed a great increase in knowledge of beta minus decay energies in the heaviest elements. These factors have led to more exact closed decay cycles which have been carefully studied by Seaborg, et al.[2] These closed cycles thus become especially useful in the calculation of electron capture decay energies.

Other methods are possible for the experimental determination of electron capture decay energy. The continuous gamma radiation accompanying electron capture has been studied in the case of Fe^{55}.[3] In the primary electron capture process, the whole energy most frequently goes with the neutrino, but may be shared between the neutrino and a gamma quantum. The upper limit of the gamma spectrum corresponds to the case when the whole disintegration

energy is taken away by the gamma quantum. Thus, from this upper limit the mass difference of the parent and the daughter atoms can be obtained directly. An apparent difficulty with this method is the large amount of radioactivity necessary before the continuous gamma spectrum can be observed, since the probability of emission of continuous gamma radiation is rather small. When positron and electron capture decay occur in the same nucleus, it is possible to determine the electron capture decay energy from the kinetic energy of the positron. This method is obviously not applicable to the heaviest elements due to the absence of detectable positron branching. Another method of measuring electron capture decay energy is the accurate determination of the (p, n) reaction threshold. This method is useful when the daughter nucleus is stable or long-lived enough to allow sufficient quantities to be available for the determination. If the (p, n) reaction threshold is known, it is a simple matter to calculate the mass difference between the parent and daughter nuclei for essentially the reverse process, in this case, orbital electron capture. However, detection of the energetic threshold for this reaction in the heaviest elements is difficult because it lies well below the value for the potential barrier between a proton and the target nucleus.

The alpha decay systematics developed by Perlman, Ghiorso, and Seaborg, have been especially useful in the discovery of new isotopes in the transuranium elements. Often, a probable mass assignment for an alpha activity of a given element may be made with the use of these systematics. In a similar fashion, it would be very

useful if electron capture half-lives and decay schemes could be predicted when searching for new isotopes in the heavy region. Furthermore, since this is the only region where the decay energy for electron capture process can be calculated and the decay studied with a fair degree of accuracy for a considerable number of cases, a study of electron capture in the heaviest elements should lead to a greater understanding of this process.

Some studies of electron capture in the heaviest elements have already been made by Thompson[4] and Feather.[5] Each author has made a plot of electron capture half-life versus energy for limited numbers of nuclides in the heavy region. From a correlation of this sort, the nuclides were grouped according to the allowed or forbidden nature of the transitions. However, these correlations were limited by a lack of experimental data for the electron capture isotopes of this region.

This investigation was therefore instigated as the beginning of a program to make a detailed study of orbital electron capture decay in the heaviest elements. Furthermore, it was seen that the data on electron capture nuclides in this region were incomplete and that a study of electron capture decay schemes was necessary before any theoretical conclusions could be made. Knowledge of the decay scheme becomes especially necessary when the decay occurs to highly excited levels of the daughter nucleus, for an accurate decay energy cannot be calculated without this information.

For each electron capture isotope, it would be desirable to obtain the following data: (1) electron capture partial half-life,

(2) mass number of nuclide, (3) decay energy of electron capture process, (4) decay scheme of electron capture decay, (5) K to L electron capture ratio, last and obviously (6) atomic number of electron capture nuclide. In a study of decay schemes, the multipole order of the gamma rays observed can be deduced if data are available on the conversion coefficients and lifetimes of the states. If these multipolarities are known, spins and parities of the levels of the daughter nucleus can also be deduced if the spin and parity assignments of the parent and daughter nuclei are available. The spin-orbit coupling model for nucleons proposed by Mayer[6] and others[7] becomes useful in this respect. In addition, certain nuclear spins have been measured in the heaviest elements.

The alpha and beta minus decays of isotopes to the same daughter nucleus as the orbital electron capture decay are often very useful in this type of study if a level scheme for the daughter nucleus can be deduced from these data. In particular, the studies by Asaro and Perlman of alpha decay have proved valuable where certain regularities have been shown to exist for excited levels of even-even nuclei.

II. EXPERIMENTAL METHODS

A. Production of Isotopes

A number of bombardments of bismuth were made to produce certain astatine isotopes. The bismuth samples to be bombarded were made by melting powdered bismuth metal onto aluminum disks in a layer approximately 1/16 inch thick. These targets were clamped in a water-cooled target holder and mounted

so as to intercept the full deflected beam of the 60-inch cyclotron of the Crocker Radiation Laboratory. A full energy beam of helium ions (38-39 Mev) was used in those bombardments where a mixture of At^{210} and At^{211} was desired, while the beam was attenuated to approximately 28 Mev with an appropriate number of one mil aluminum foils when At^{211} alone was desired.[8] The helium ion beam was limited to 15 microamperes to prevent overheating of the target and subsequent loss of astatine by volatilization.

The bombardment and safe handling of alpha radioactive materials in the cyclotron present further problems not encountered with the bismuth targets. To facilitate this type of bombardment a special target assembly, a pistol-grip target holder, has been designed which is described elsewhere.[9] Uranium, enriched U^{233} and U^{235} isotopes, and neptunium (Np^{237}) were used as target materials. The uranium isotopes were bombarded as ammonium uranyl phosphate and, in some cases, uranium oxide, slurries of which were evaporated in the platinum holders.[10] The U^{233} was bombarded with 36 Mev helium ions to produce Pu^{234} by means of an (α, 3n) reaction. The U^{235} was bombarded with 36 Mev helium ions to produce Pu^{237} by means of an (α, 2n) reaction and with 19 Mev deuterons to produce Np^{234} by means of a (d, 3n) reaction in separate bombardments. The neptunium target material was precipitated in the form of the fluoride, NpF_4, and evaporated in the platinum holder. A bombardment of this neptunium with 9.5 Mev protons produced Pu^{237} by means of a (p, n) reaction.

Am^{241}, in the form of americium oxide which had been

previously purified, was irradiated with slow neutrons for a five-day period in the MTR reactor at the Reactor Testing Station, Arco, Idaho. The desired products were a pair of isomers of Am^{242} produced by the (n, γ) reaction.

B. Chemical Procedures

Original experiments by Corson, et al.[11] and later work by Johnson, et al.[12] indicated that astatine is quite volatile when in the zero valence state. The isolation of the astatine from the bismuth targets was accomplished using a rapid separation which employed the high volatility of astatine as compared to polonium, bismuth, and lead. The method and apparatus have already been described in other work on isotopes of astatine.[13] The purity of the vaporized astatine samples was checked by alpha and gamma pulse analysis.

The neptunium and plutonium radioactivities were separated from the uranium and neptunium targets and purified by using a combination of precipitation and ion exchange methods devised by Orth.[10]

The neutron-irradiated americium oxide was dissolved in HCl. A small portion of the total solution was removed and treated to separate and purify the americium. To accomplish this, fluoride and hydroxide precipitations were carried out and a 13 M HCl cation (Dowex-50) ion exchange column[9] was used to separate rare earth fission products. Then the americium was oxidized to the hexapositive oxidation state using persulfate ion in an acid medium,[9,14] the curium being removed as a fluoride precipitate, leaving purified americium. The americium was reduced with hydrazine

and precipitated as a fluoride, then a hydroxide. A small part of this material (a number of micrograms) was dissolved in HNO_3 to be used to prepare a sample for the beta ray spectrometer. The remainder was converted to americium oxide by heating and mounted in the bent crystal gamma ray spectrometer. The whole procedure was carried out as rapidly as possible to reduce the loss of 16-hour Am^{242m} by decay.

C. Instruments Used to Measure Radiation

Radioactive decay of samples was followed on a counter using an Amperex Geiger tube filled with a chlorine-argon mixture connected to a standard scaler. A windowless proportional counter with a continuous methane flow was also used for measuring sample decay. This instrument was particularly useful because of the favorable counting efficiency for electron capture isotopes. Hulet[15] has found the counting efficiencies of certain electron capture nuclides to vary between 30 - 45 percent. Decay of alpha emitting nuclei was also measured with an argon filled ionization chamber, which has a counting yield of 52 percent, connected to a standard scaler.

Samples of alpha emitters were counted in a 48-channel differential alpha particle pulse analyzer[16] where discrimination of energies was desired. Accurate determinations of the alpha particle energies of At^{210}, At^{211}, and Po^{211} were made using an alpha particle spectrograph.[17] The astatine samples, collimated in the form of a 1 x 1/8 inch slit, were vaporized directly from the target onto a 2 mil platinum plate for mounting in the spectrograph.

Essentially mass free samples were prepared by this method.

The pulse analysis of gamma rays and x-rays was accomplished using a sodium iodide (thallium activated) crystal detector, 1 x 1 1/4 in. diameter, sealed to a Dumont 6292 photomultiplier tube. The pulses from the photomultiplier were amplified and were sorted according to energy in a 50-channel differential pulse analyzer of new design utilizing 6BN6 tubes in a "snapper" type of circuit.[18] The counting efficiency of a sodium iodide crystal of these dimensions has been determined.[19] In the lower energy regions (<150 kev) the escape peak resulting from the loss of iodine K x-rays from the crystal became important when calculating abundances. The escape peak was observed at 29 kev lower in energy than the photoelectric peak and in approximately 10 - 15 percent abundance for K x-rays in the 100 kev region. The gamma rays of Am^{241} and U^{235} served as standards below 200 kev while those of Na^{22}, Cs^{137}, and Co^{60} were used for energy calibration in the higher energy regions. L x-rays and gamma rays in the 10 - 60 kev range were measured using a xenon-filled (90 percent xenon and 10 percent methane at one atm.) proportional counter connected to the 50-channel pulse analyzer. The L x-rays of the elements studied were resolved into L_α, L_β, and L_γ x-rays, the L x-rays of neptunium associated with the alpha decay of Am^{241} being used as standards.

Analyses of conversion and Auger electron lines were made with the aid of a double focusing, $\pi\sqrt{2}$, magnetic beta ray spectrometer.[20] The instrument was calibrated using the end-points of the Pu^{241} and P^{32} beta spectra and the conversion lines from gamma rays in Cs^{137} and I^{131}. The Am^{242m} samples were evaporated onto

aluminum leaf (177 micrograms/cm^2) while the astatine samples were vaporized onto 0.25 mil platinum foil, good results being obtained even with this thick backing material. The counter window in the spectrometer was made of a thin film of vinyl plastic which stopped all electrons <3-5 kev. No window absorption corrections were made for abundance calculations since the energies of electron groups were >15 kev.

The L x-rays and gamma spectrum of Am^{242m} were measured in a bent crystal gamma ray spectrometer of the Cauchois type, previously described by Barton, et al.[21] and modified further by Browne.[22] Mounting of the sample, approximately 1.5 mg of americium, was done by standard methods described in the above mentioned reports.

III. EXPERIMENTAL RESULTS

A. Astatine 211

Astatine 211, the first isotope of the element astatine to be identified, was produced by Corson, et al.[11] in bombardments of bismuth targets with 32 Mev helium ions. Two alpha groups and electromagnetic radiation with an energy around 90 kev were observed to decay with a 7.5-hour half-life. They suggested that one of the alpha groups belonged to AcC' (Po^{211}) and that the 7.5-hour activity was At^{211} which showed branching decay, 60 percent electron capture to Po^{211} and 40 percent alpha emission to Bi^{207}, the decay of which had not yet been observed. The branching of At^{211} has subsequently been measured to be 59.1 percent electron capture and 40.9 percent alpha emission by Neumann and Perlman.[23]

Further experiments by Corson, et al.[24] proved by critical absorption methods that the electromagnetic radiation was polonium

K x-rays. They also observed soft x-rays whose absorption coefficient in aluminum was consistent with that of L x-rays of polonium. The decay of At^{211} may be shown diagrammatically in the following manner:

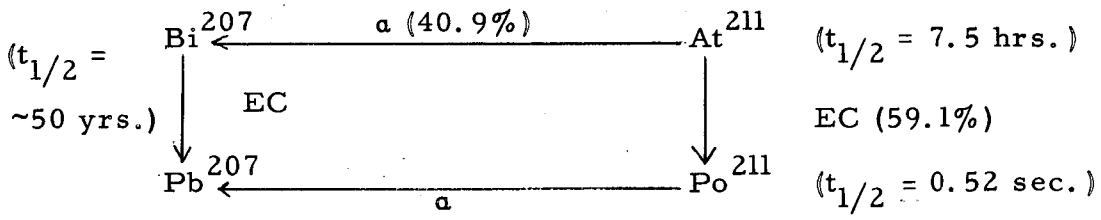

The half-life of the Po^{211} daughter is 0.52 seconds[25] and is, therefore, in equilibrium with the At^{211}, while the Bi^{207} daughter has a half-life which is long enough (~50 yrs.)[23] that it may be neglected when working with active samples of At^{211}. The ultimate product, Pb^{207}, is a stable isotope.

A careful search has been made by the author for gamma rays other than the polonium x-rays using a differential pulse analyzer connected to a sodium iodide crystal detector and a xenon-filled proportional counter. No other electromagnetic radiation has been found allowing an upper limit of 0.5 percent of the total disintegrations to be set for the abundance of any possible gamma ray present with the exception of radiations with energies identical to those of polonium x-rays. These data indicate that the electron capture decay of At^{211} proceeds directly to the ground state of the daughter nucleus utilizing the maximum energy available for the transition.

Abundances of the K and L x-rays of polonium produced in the decay of a sample of At^{211} have been measured. From this

information a ratio of K to L shell vacancies can be calculated directly when the necessary corrections have been made for the Auger effect associated with the K and L x-rays. Germain[26] has studied experimentally the Auger effect for the K electron capture of At^{211}. His result for the Auger coefficient, which is defined as the number of Auger electrons per K shell vacated, is 0.106. For the L x-rays experimental data are available only for the fluorescence yield (which is one minus the Auger coefficient) of the L_{III} levels.[27] However, Kinsey[28] has been able to calculate fluorescence yields of the L_I and L_{II} levels from a consideration of experimental data on total level widths combined with theoretical radiation widths for these levels. If one uses fluorescence yield values for bismuth as given by Kinsey (he has shown that fluorescence yield varies slowly as a function of Z), an effective fluorescence yield of 0.35 for the L_α, L_β, and L_γ x-rays of polonium is obtained.

It is possible for an Auger transition to occur in which a vacancy is shifted from one L level to another and a doubly ionized atom is produced by ejection of an electron from a level of lower energy. This effect is called a Coster-Krönig transition. Kinsey has suggested that the most frequent double ionizations are vacancies in L_{III} and either M_{IV} or M_V shells created by Auger transitions from the L_I shell. His estimate of the magnitude of this effect, 70 percent of all L_I vacancies, in bismuth is in poor agreement with the experimental results of Browne.[22] For the present calculations, the Coster-Krönig effect will be neglected for lack of data on its relative importance.

The data obtained on At^{211} using the xenon proportional counter show the relative intensities of L x-rays to be:

$$L_\alpha : L_\beta : L_\gamma = 1.0 : 1.0 : 0.4.$$

Combining this with the K x-ray abundance from the sodium iodide crystal spectrometer, a K to L x-ray ratio of 3.1 is calculated. Correcting these values for Auger effect, the data yield a ratio of 1.2 for the K to L shell vacancies. Assuming 70 percent of the K vacancies are filled from the L shell (deduced from intensity data), a K to L electron capture ratio of approximately 7 is obtained.

The Auger electron spectrum of astatine 211 has been determined on a beta ray spectrometer and is shown in Figure 1. Four peaks are easily discernible at 56.9, 60.1, 70.5, and 73.7 kev, while other perturbations of the spectrum in this energy region are also visible. There is a rather ill-defined electron peak at very low energy (<10 kev). However, the resolution of definite electron groups in this region is very difficult. No other features of the spectrum were evident in scanning up to higher energies. The two lowest energy electron groups have energies consistent with assignment to K-LL Auger electrons, while the two highest energy electron groups can be assigned to K-LX Auger electrons (where X denotes M, N, etc. shells). A possible third group is visible at 84 kev whose energy is consistent with that of K-XY Auger electrons (where Y also denotes M, N, etc. shells). The ratio of these three Auger electron groups was found to be K-LL:K-LX:K-XY = 1.0:0.4:0.04. This result is in poor agreement with a K-LL:K-LX ratio of 1.00:0.71 obtained by Broyles, et al.[29]

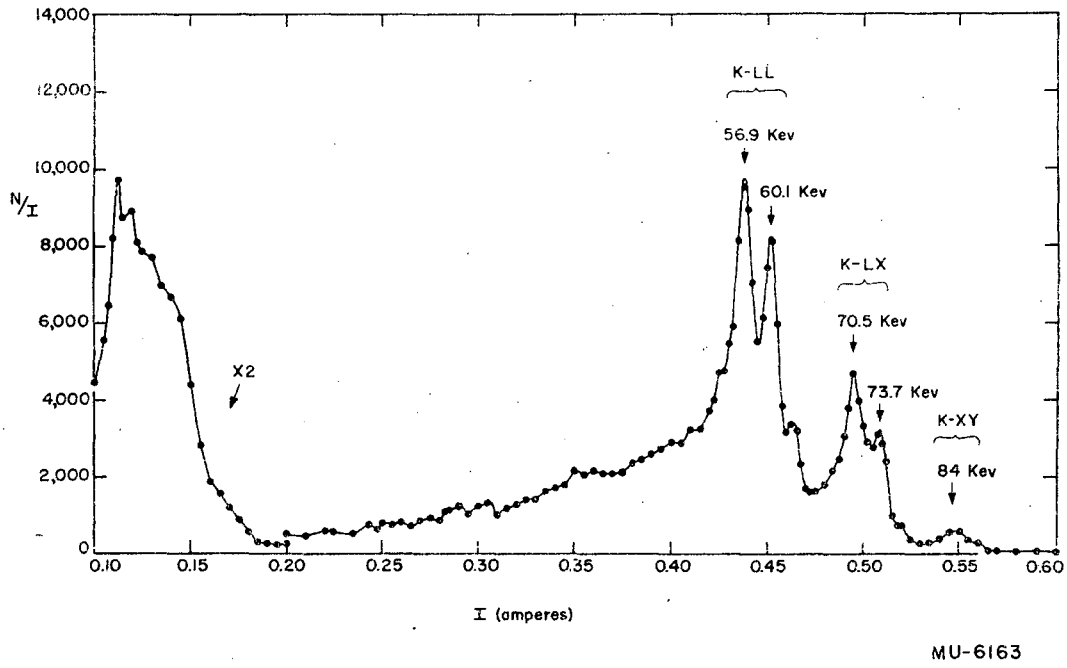

Fig. 1. Auger electron spectrum of At^{211}.

for mercury. Using two isotopes of platinum, Steffen, et al.[30] determined average ratios of K-LL:K-LX:K-XY = 1.00:0.86:0.025. Ellis[31] and Flammersfeld[32] have measured the relative intensities of several of the Auger lines for bismuth using 180 degree magnetic spectrometers. Ellis reports the K-LX to K-LL ratio to be greater than 0.4 while Flammersfeld reports it is at least 0.57.

The alpha spectrum of At^{211} was studied in an alpha ray spectrograph. Only one group of alpha particles was observed with an energy of 5.862 Mev determined against Am^{241} and Po^{218} standards. Ion chamber measurements had yielded energies of 5.85 [33] and 5.89 [34] Mev.

Experimental data on the decay of At^{211}, Po^{211}, and Bi^{207} allow the electron capture energy of At^{211} to be estimated.[2] The crucial point in this closed cycle is the estimation of Bi^{207} electron capture energy. The relatively long, 50-year half-life of Bi^{207} indicates very little transition energy, while Neumann and Perlman[23] have observed conversion electrons from gamma rays in Bi^{207} decay as energetic as 2.49 Mev. These data suggest an energy difference of approximately 2.50 Mev between Bi^{207} and Pb^{207}, with a probable energy of 0.90 Mev and a minimum of 0.89 Mev available for the electron capture of At^{211}.

B. Polonium 211

Polonium 211, an alpha emitter with a 0.52-second half-life, exists in equilibrium with At^{211} from the 59.1 percent electron capture branching of this astatine isotope. Neumann and Perlman[23] have reported three low-abundance alpha groups at 6.90 (0.6 percent),

6.57 (0.5 percent) and 6.34 Mev (0.1 percent) in addition to the main alpha group at 7.34 Mev. The first two of these groups have been observed using the alpha ray spectrograph at 6.895 (0.50 percent) and 6.569 Mev (0.53 percent). No alpha group corresponding to the reported group at 6.34 Mev has been seen between 6.26 and 6.57 Mev which is more than 0.02 percent abundant with respect to the main alpha group.

C. Astatine 210

Astatine 210 was first reported by Kelly and Segrè[8] to have a half-life of 8.3 hours and decay by electron capture with emission of a gamma ray of approximately 1.0 Mev energy. Neumann, et al.[35] have shown the existence of a slight amount of alpha branching in the decay of this isotope by separating the alpha daughter, Bi^{206}.

The gamma ray spectrum of a mixture of At^{210} and At^{211} was measured with a sodium iodide crystal gamma ray spectrometer. The results are shown in Figures 2a and b. In addition to the K x-rays of polonium, three gamma rays are seen with well-defined peaks at 0.24, 1.19, and 1.46 Mev energy. After correction for the counting efficiencies of the gamma rays in the sodium iodide crystal,[19] the following relative abundances were calculated:

$$\text{K x-rays: } \gamma_1(0.243) : \gamma_2(1.19) : \gamma_3(1.46) =$$
$$1.00 : 0.33 : 0.47 : 0.26.$$

The K x-ray abundance is not too significant since it represents contributions from the electron capture of a mixture (probably about 2:1) of At^{210} and At^{211}, respectively.

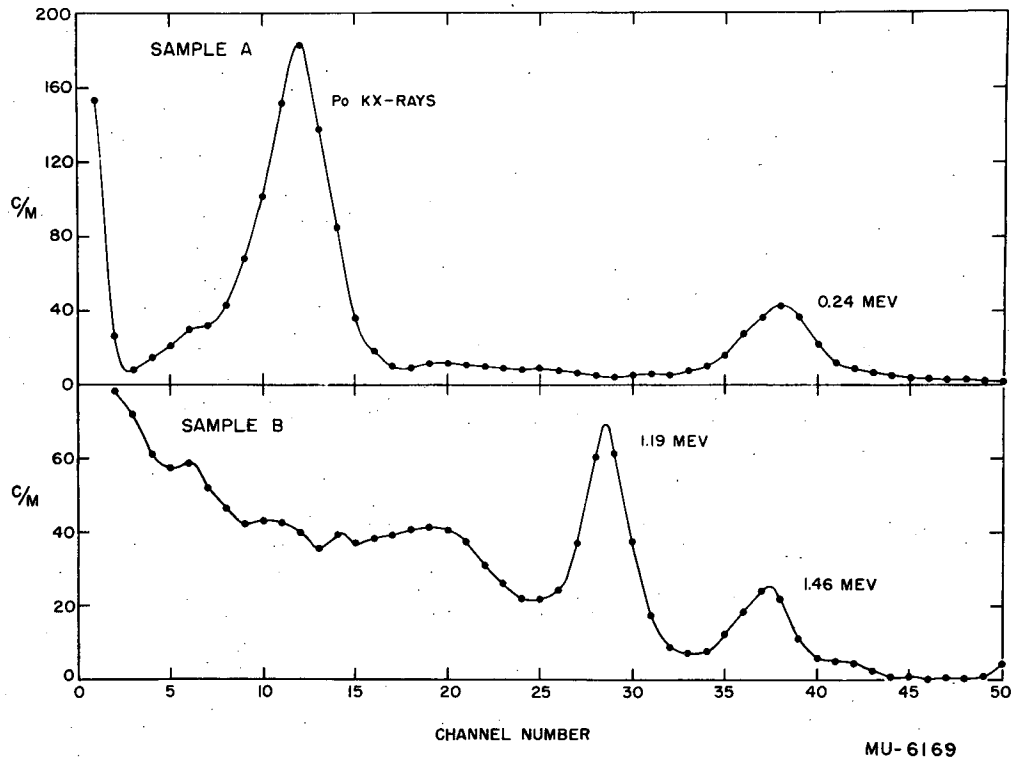

Fig. 2a. Gamma ray spectrum of $At^{210-211}$.

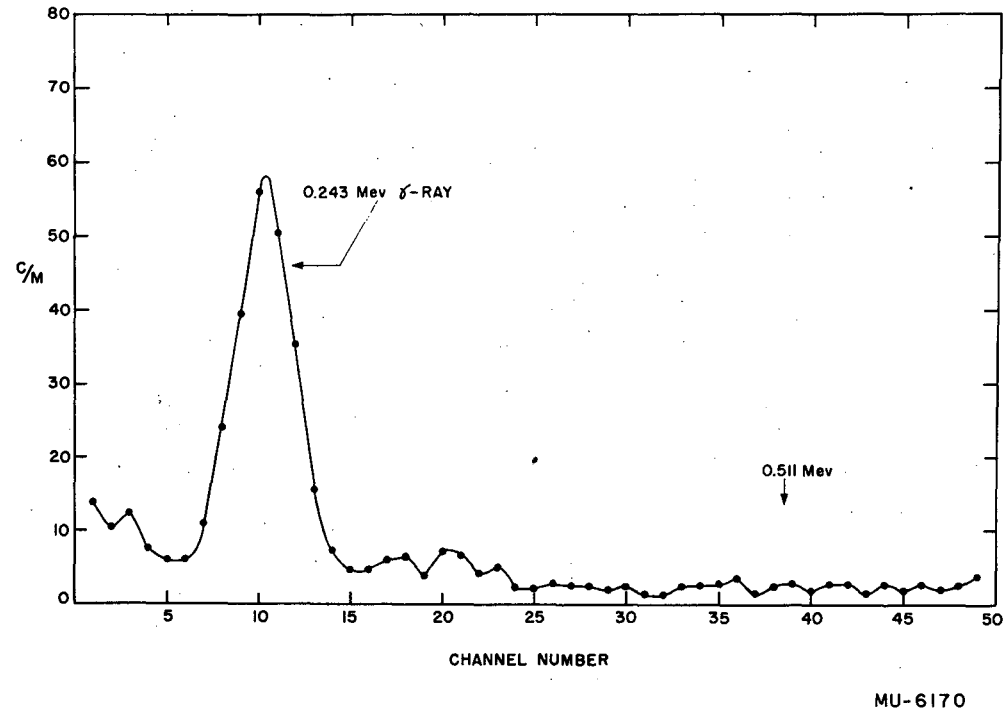

Fig. 2b. Gamma ray (243 kev) of At^{210}.

The conversion electron spectrum of the astatine mixture has been determined in the beta ray spectrometer. At this point the knowledge of the Auger electron spectrum of At^{211} proved particularly valuable in determining which electron lines of the mixture were due to At^{210}. The electron spectrum of the mixture is shown in Figures 3a, b, and c, at different times. Conversion electrons from six different gamma rays have been resolved. Data on these radiations are shown in Table 1. In most of the cases, except for the 44.6 kev gamma ray, the energy of the gamma ray has been determined principally from the K conversion electron line due to the lack of ambiguity in interpretation. The L and M conversion lines, when present, have served as a further calibration of the energy assigned to the gamma ray. In the case of the 44.6 kev gamma ray, the best energy determination was made from the L_{III} conversion line which is clearly resolved. The electron peak at 27.4 kev could be an L_I or L_{II} conversion line or, more likely, a mixture of both. Energetically the best assignment of this line would be to the L_I conversion electrons. The two conversion electron peaks in the 1.36 - 1.41 Mev region prove the existence of two energetic gamma rays with a difference between them of 46 kev, both of which were first observed together as one peak at 1.46 Mev in the gamma spectrum. Observation of the conversion electrons from the 44.6 kev and 115 kev gamma rays stimulated a search for these radiations. A gamma ray at approximately 46 kev was observed using the proportional counter (see Figure 4), but it has not been possible to resolve

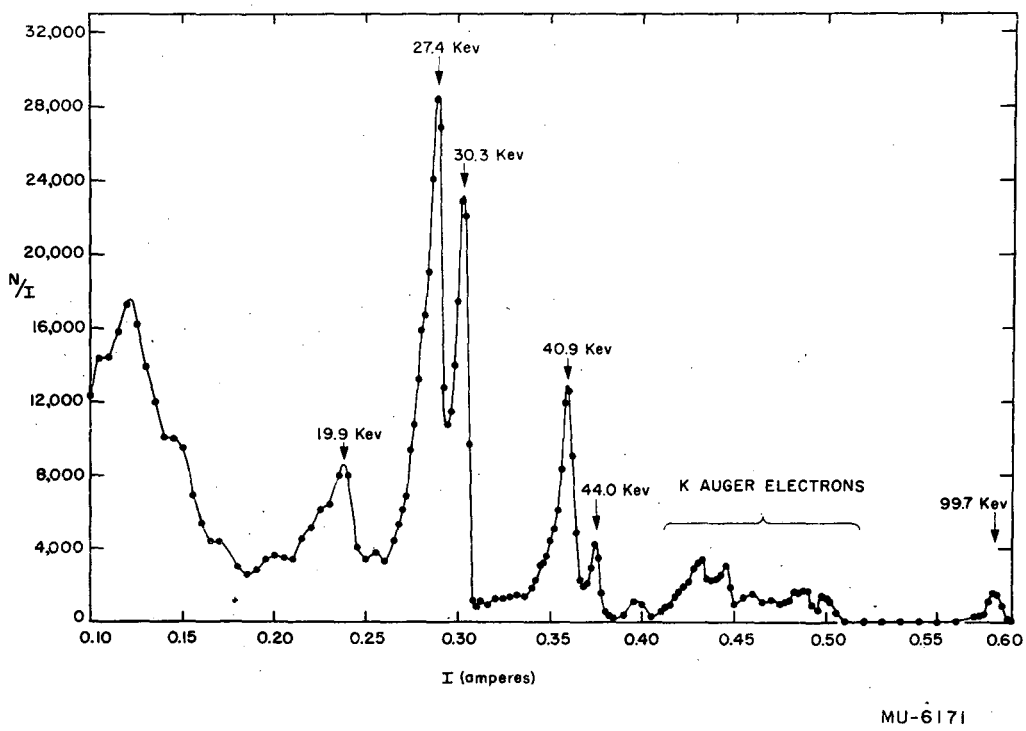

Fig. 3a. Auger and conversion electron spectrum of $At^{210-211}$.

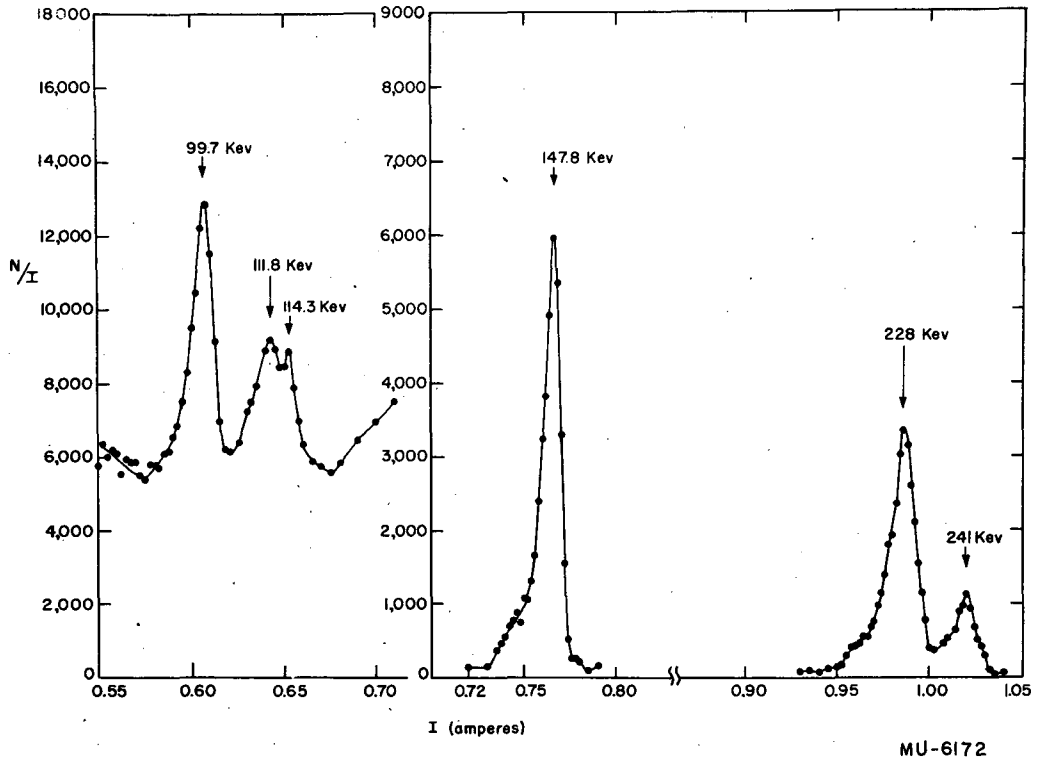

Fig. 3b. Conversion electron spectrum of $At^{210-211}$.

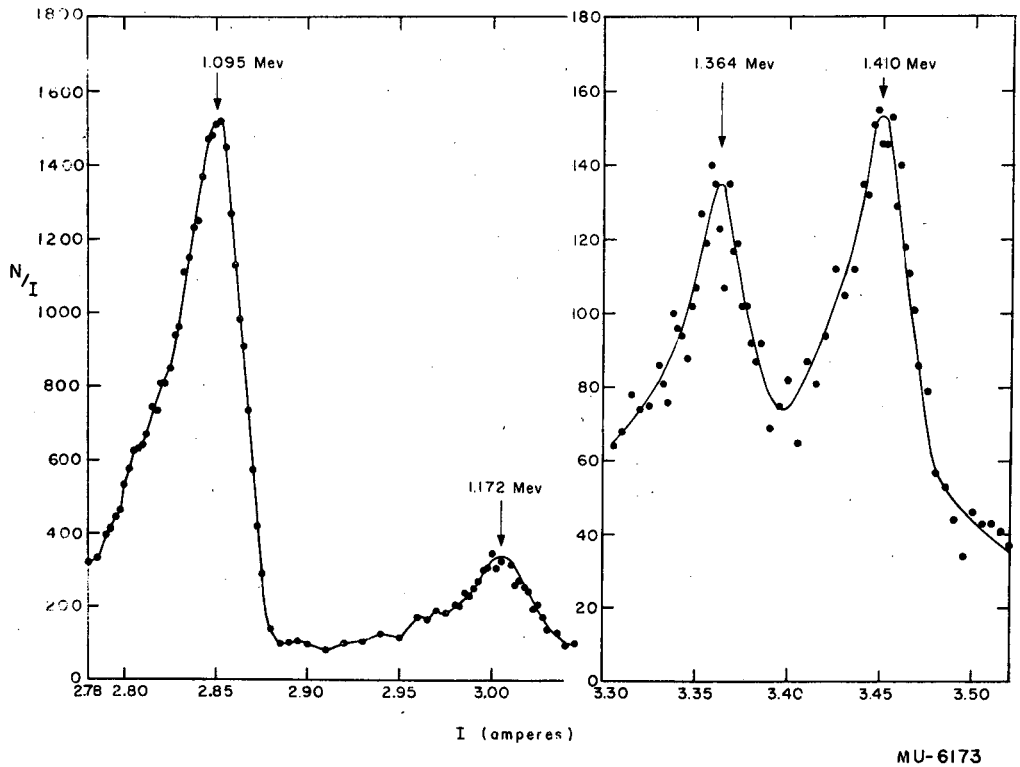

Fig. 3c. Conversion electron spectrum of $At^{210-211}$.

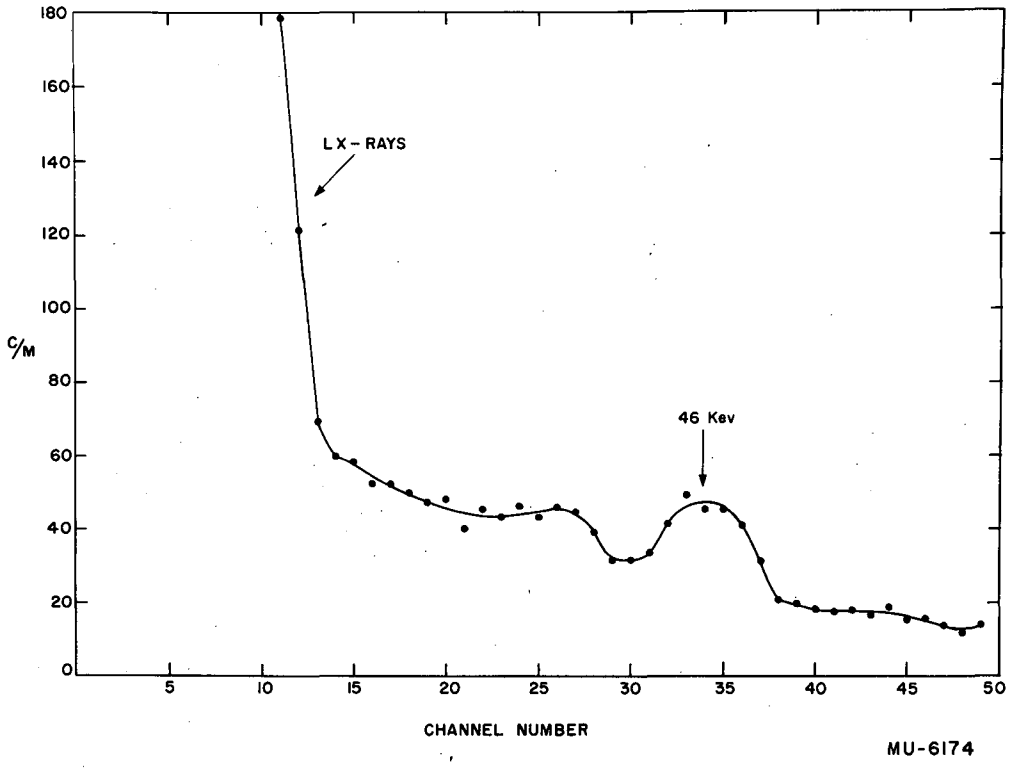

Fig. 4. Radiation (45 kev) of At^{210} (xenon proportional counter).

Table 1

Gamma Ray (Mev)	Conversion Shell	Electron Energy (Mev)	Conversion Electron Ratio	K Conversion Coefficient
0.0446	L_I or L_{II}	0.0274	$L_I + L_{II}$:L_{III}:M:N = 1.00:0.48:0.41:0.10	
	L_{III}	0.0303		
	M	0.0409		
	N	0.0440		
0.115	K	0.0199	K:L:M + N = 1.00:0.17:0.14	
	L	0.0997		
	M	0.1118		
	N?	0.1143		
0.243	K	0.1478	K:L:M + N = 1.00:0.83:0.25	1.1×10^{-1}
	L	0.228		
	M	0.241		
1.189	K	1.095	K:L = 1.00:0.21	4.8×10^{-3}
	L	1.172		
1.458	K	1.364		1.2×10^{-3}
1.504	K	1.410		

L : K : K : K : K = 1.00:0.25:0.27:0.015:0.0021
0.0446 0.115 0.243 1.19 1.46 + 1.50

a 115 kev gamma ray from the K x-rays of polonium at 85 kev, probably because of the low intensity of the gamma ray.

The K/L conversion ratios for the 0.115, 0.243, and 1.19 Mev gamma rays have been compared with empirical plots of K/L conversion versus Z^2/E prepared by Goldhaber and Sunyar.[36] For the 0.115 Mev gamma ray, the experimental ratio falls midway between values for M1 and M2 transitions and with the present data, a choice between the two cannot be made. In the case of the 0.243 Mev gamma ray, the experimental ratio can be correlated with empirical values for E2 or M4 transitions. The E2 assignment is preferred in the tentative decay scheme that will be shown. While Goldhaber and Sunyar have no data for the 1.2 Mev region, an extrapolation of their empirical K/L conversion ratios would favor an E3 assignment to the 1.19 Mev gamma ray. The $L_I + L_{II}/L_{III}$ conversion ratio for the 44.6 kev gamma ray has been compared with the theoretical L conversion coefficients calculated by Gellman, et al.[37] using relativistic non-screened electron wave functions. The calculations were made for E1, M1, and E2 transitions with $L_I + L_{II}/L_{III}$ ratios of 1.6, 1000, and 1.0, respectively. The experimental value of 2.1 shows the best agreement with that for an E1 transition.

Conversion coefficients for the K shell have been calculated using the data on electron and gamma ray abundances in a given sample for the 0.243, 1.19, and 1.46 + 1.50 Mev gamma rays. These K conversion coefficients have been compared with theoretical values calculated by Rose.[38] The conversion coefficients

for the 0.243 and 1.19 Mev radiations correlate with theoretical values for E2 transitions. In the case of the first gamma ray, a definite assignment is made from the E2 or M4 predictions of the K/L conversion ratio correlation. Similarly, the 1.19 Mev gamma ray was thought to be an E3 transition from its K/L conversion ratio, but the K conversion coefficient may be considered a better criterion and the E2 assignment made definite. This 1.19 Mev transition is thought to arise from the decay of the first excited state to the ground state since experimental data indicate the spacing of the first excited level above the ground state should be around 1 Mev in the region of the closed shell of 126 neutrons. In almost all cases studied so far, the first excited state of an even-even nucleus has shown spin 2 and even parity and decays to the ground state (spin zero with even parity) by an E2 transition.[39] These data also suggest the 1.19 Mev gamma ray to be an E2 transition with a spin assignment of 2 with even parity for this level. A combined K conversion coefficient calculated for the 1.46 and 1.50 Mev gamma rays has a value that can best be correlated with an E1 transition.

A suggested decay scheme for the levels of Po^{210} is given in Figure 5. The 0.115 Mev transition, present in low abundance, has not been assigned in the scheme shown. The spin and parity assignments to the two highest levels are tentative. The discrepancy in energy between the 0.243 Mev gamma ray and the 0.269 Mev difference between the first and second levels is not considered large enough to warrant assignment of any additional levels to the

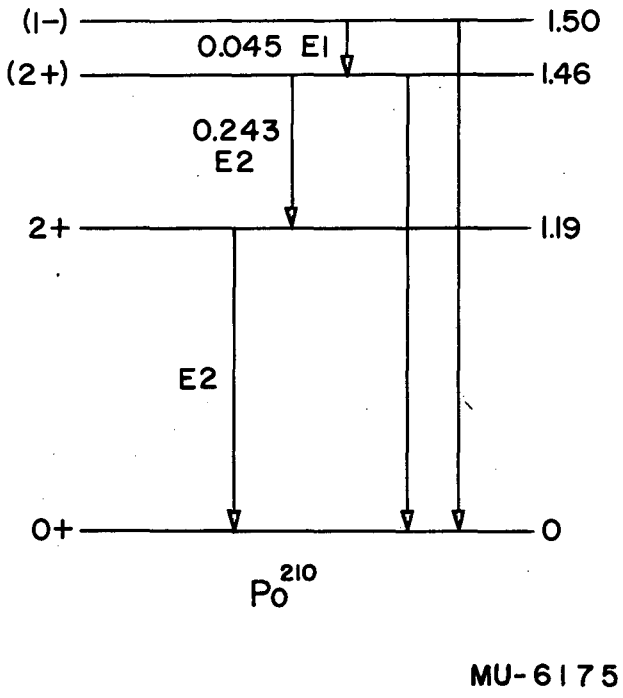

Fig. 5. Level scheme of Po^{210} from At^{210} decay.

Po^{210} nucleus. The 2+ assignment to the level at 1.46 Mev is consistent with the E2 assignment to the 0.243 Mev gamma ray and with the presence of a cross-over transition to the ground state. The 0.243 Mev gamma ray is most likely an M1 - E2 mixture with E2 apparently predominating. A spin of one with odd parity is suggested for the level at 1.50 Mev from the assignment of electric dipole radiation to the 45 kev gamma ray and from the cross-over decay of this level to the ground state. Although one might expect decay from this 1- level to the 2+ level at 1.19 Mev, it has not yet been detected. This level scheme is consistent with the absence of gamma rays in the beta decay of Bi^{210} which has only 1.17 Mev decay energy. Electron capture can be occurring to any of these levels, but the large amount of gamma radiation present suggests that much of the decay takes place to the uppermost state at 1.50 Mev. The large amount of internal conversion precludes the calculation of an accurate K/L electron capture ratio from the x-ray abundances.

The alpha particles from the decay of At^{210} have been observed in two different runs on the alpha ray spectrograph. Three alpha groups have been observed at 5.519 (32 percent), 5.437 (31 percent), and 5.355 (37 percent) Mev. A graph of the spectrum of a mixture of At^{210} and At^{211} is shown in Figure 6. Two other possible groups in lower abundance are seen as shoulders on the high energy sides of the 5.355 and 5.437 Mev peaks. The energies have been calculated using the Po^{210} present as an internal standard. It is also possible to calculate the alpha branching ratio using this

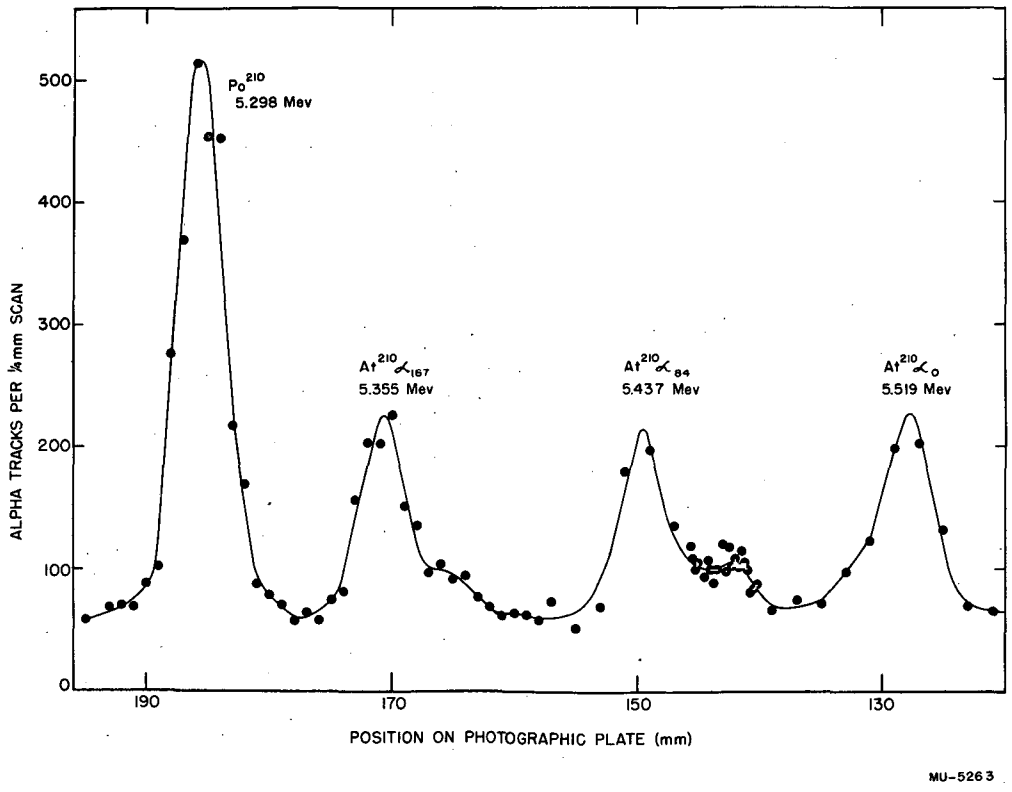

Fig. 6. Alpha particle spectrum of At^{210}.

Po^{210} peak as a measure of At^{210} electron capture decay. A branching of 0.17 percent was found for the alpha decay of At^{210}.

Unfortunately, the closed decay cycle At^{210}-Po^{210}-Pb^{206}-Bi^{206} does not yield the electron capture decay energy of At^{210} because the decay energy of Bi^{206} is unknown, nor are any heavier members of the cycles containing At^{210}-Po^{210} useful. Therefore, the information on the decay of At^{210} does not contribute greatly to furthering our knowledge of the electron capture process. One point to be mentioned is the favoring of the apparent 1- state by the decay of the At^{210} nucleus in preference to decay to even parity states with low spin where more energy is available. An odd parity assignment to the astatine nucleus suggested by these data is consistent with predictions of the Mayer shell model for 85 protons - 125 neutrons. Furthermore, the data gained on the spacing of levels at 126 neutrons is of value, and, along with Tl^{208} - Pb^{208} decay, is the only information available on the excited levels of nuclei at this closed shell.

The existence of gamma rays with as much as 1.5 Mev energy demonstrates that positron emission is a possible means of decay for the At^{210} nucleus even though the actual decay energy cannot be calculated from closed decay cycles. However, good evidence for lack of positron decay in this isotope is shown in the gamma spectrum (Figure 2b) where no annihilation radiation is observed at 0.511 Mev. An upper limit of 5 percent may be set for positron branching in At^{210}. The electron capture decay to a highly excited state of Po^{210} is probably utilizing less than the

minimum energy (1.02 Mev) required for positron emission, and selection rules apparently do not permit competition by positron decay to the lower states of Po^{210}.

D. Neptunium 234

Neptunium 234 was first observed by James, et. al.[40] in a bombardment of U^{235} with deuterons, and later observed in bombardments of U^{233} with deuterons[41] and of Pa^{231} with helium ions.[42] It was shown to be an electron capture isotope of 4.4 day half-life with an associated gamma ray of 1.9 Mev energy determined from absorption data. Further work on this isotope by Orth[10] and O'Kelley[20] has shown evidence for gamma rays with energies 0.177, 0.442, 0.803, and 1.42 Mev determined from the conversion electron spectrum. They reported a K/L electron capture ratio of approximately one.

Although the uranium bombardments done by the author did not produce enough Np^{234} activity to allow examination of the electron spectrum on the beta ray spectrometer,[20] the x-rays and gamma rays of this isotope have been studied using the xenon proportional counter and the sodium iodide crystal spectrometer. In addition to K x-rays of uranium, two definite peaks were seen in the gamma spectrum at 0.78 and 1.57 Mev, with an additional possible gamma ray in the 0.20 - 0.25 Mev region. A graph of the gamma spectrum of Np^{234} is seen in Figure 7. There was no indication of any radiation at 0.177 or 0.442 Mev, contrary to previous results. Upon replacing the sodium iodide crystal with one of anthracene, evidence was found for conversion electrons from the 0.78 Mev

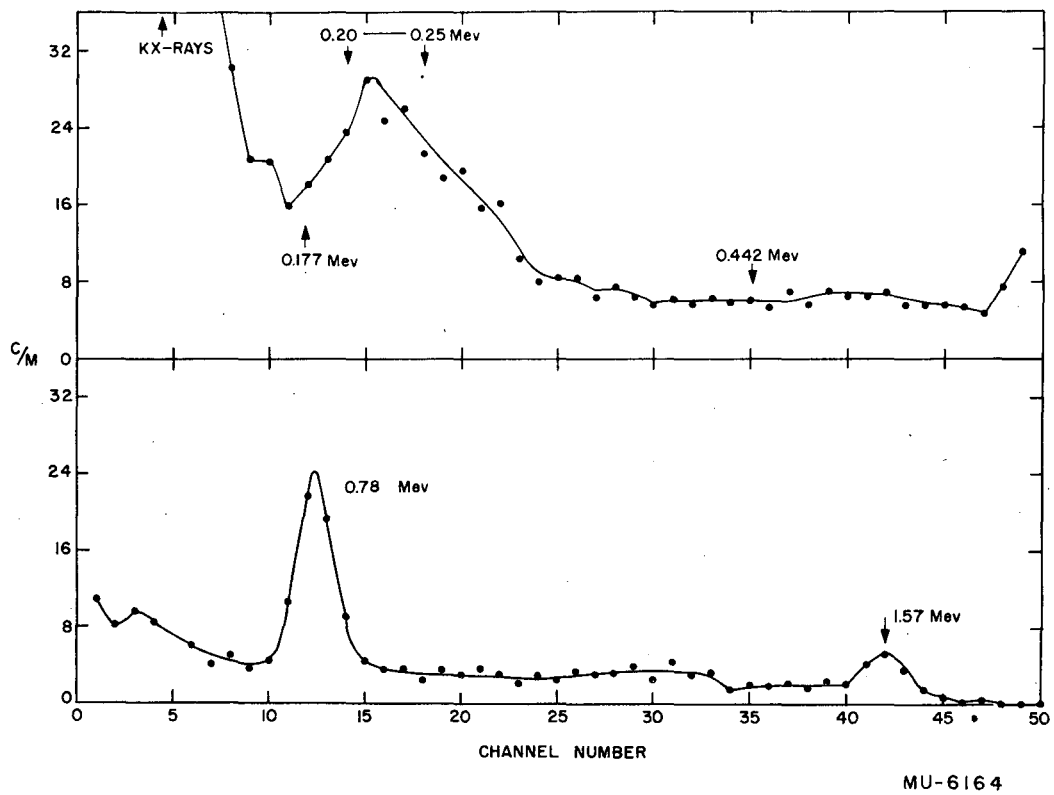

Fig. 7. Gamma ray spectrum of Np^{234}.

gamma ray, but no conversion electrons from the 0.177 or 0.442 Mev gamma rays were seen in appreciable abundance. It must be concluded that if these gamma rays do exist, they are in low abundance and may be highly converted. Combining these data on the gamma rays with L x-ray abundances measured with the xenon proportional counter, the following relative abundances were calculated:

$$\text{K x-rays} : \text{L x-rays} : \gamma_1(0.78\ \text{Mev}) : \gamma_2(1.57\ \text{Mev}) =$$

$$1.0 : 0.7 : 0.5 : 0.4.$$

The beta decay of Pa^{234} and alpha decay of Pu^{238} give some indication of the level scheme of U^{234} and are useful in interpreting the electron capture decay of Np^{234}. The first two excited states observed in U^{234} are populated by the alpha decay of Pu^{238}. From the work of Asaro,[43] these levels are 0.043 and 0.146 Mev above the ground state. The first excited state is thought to have spin 2 with even parity while the spin of the second excited state is probably 0, 2, or 4 with even parity. The experimental data on the two isomers of Pa^{234}, UX_2 and UZ, have been tabulated in the Table of Isotopes.[44] More recent work on UX_2 has been reported by Stoker, et.al.[45] The beta spectrum of UX_2, with three groups at 2.31 Mev (90 percent), 1.50 Mev (9 percent), and 0.58 Mev (1 percent), indicates excited levels of U^{234} at 0.81 Mev and approximately 1.7 Mev. The beta spectrum of UZ containing two groups at approximately 1.2 Mev (10 percent) and 0.45 Mev (90 percent) indicates a level separation of 0.75 Mev. The difference between the most energetic beta groups of each

isomer together with a spacing of 0.30 Mev between the isomers suggests the beta decay of UZ is populating levels at 0.81 Mev and 1.57 Mev above the ground state of U^{234}. Evidence for cascade decay of the 1.57 Mev level though the 0.81 Mev level is shown by the observed γ-γ coincidences in the 0.8 Mev region in a sample of UZ.

A proposed decay scheme for Np^{234} is shown in Figure 8. The majority of the electron capture decay of Np^{234} proceeds to the 1.57 Mev level of U^{234} as indicated by the relative x-ray and gamma ray abundances. The peak seen in the gamma spectrum of Np^{234} at 0.78 Mev probably consists of a mixture of 0.76 and 0.81 Mev radiations resulting from the cascade decay of the 1.57 Mev level through the 0.81 Mev level. Since conversion coefficients for these high energy gamma rays, 0.78 and 1.57 Mev, are small, even for large spin changes, a fairly accurate K to L electron capture ratio may be calculated from the K and L x-ray abundances. The fluorescence yield for K x-rays of uranium may be taken as approximately 0.95, from the data of Germain[26] and Browne.[22] From the semi-empirical data of Kinsey, an effective fluorescence yield of 0.40 is obtained for the L_α, L_β, and L_γ x-rays of uranium. Taking these corrections into consideration and assuming 70 percent of the K vacancies are filled by L electrons, the result is a K to L electron capture ratio of 1.0. This may be considered an upper limit as conversion of the gamma rays would tend to reduce this value. The total electron capture energy available for Np^{234} is 1.82 Mev according to the closed decay

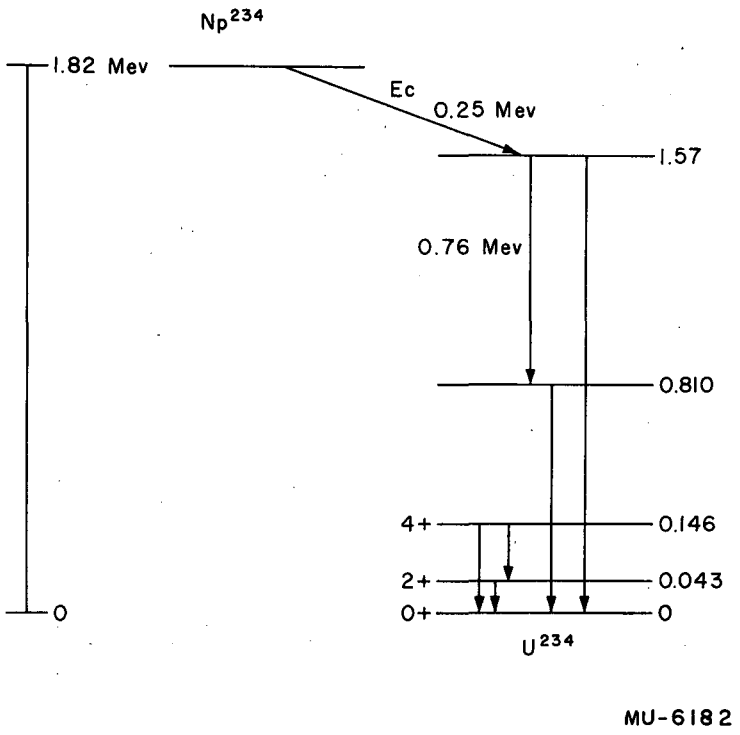

Fig. 8. Decay scheme of Np^{234}.

cycles compiled by Seaborg, et al.[2] The electron capture of Np^{234} is similar to the beta decay of UZ, in that the higher levels of U^{234} are populated in preference to the even parity states of low spin where more transition energy is available for the electron capture process. A possible explanation for this preference may be a high spin value for Np^{234} and odd parity as predicted by the Mayer shell model.

E. Neptunium 235

Neptunium 235 was first observed in the same bombardments as Np^{234}, deuteron irradiations of U^{235} by James, et al.[40] The half-life was shown to be approximately 400 days and the mode of decay presumed to be orbital electron capture. Later work by James and co-workers[46] resulted in the examination of alpha particles emitted by this isotope whose energy is 5.06 Mev with an abundance of 5×10^{-3} percent. The half-life was measured to be 410 days and an L to K electron capture ratio of >9 was reported.

A sample of approximately 10^6 disintegrations per minute of Np^{235}, produced by the method mentioned above, was obtained from Dr. S. G. Thompson for this investigation. Using a sodium iodide scintillation spectrometer, a 66 kev gamma ray was detected in addition to the K x-rays of uranium. Figure 9 shows the gamma ray resolved from the x-rays plus escape peak. Observation of the low energy radiation of this isotope with a xenon proportional counter confirmed the energy of the gamma ray and yielded the abundances of the L x-rays. The x-rays and gamma rays were measured to be in the following ratios:

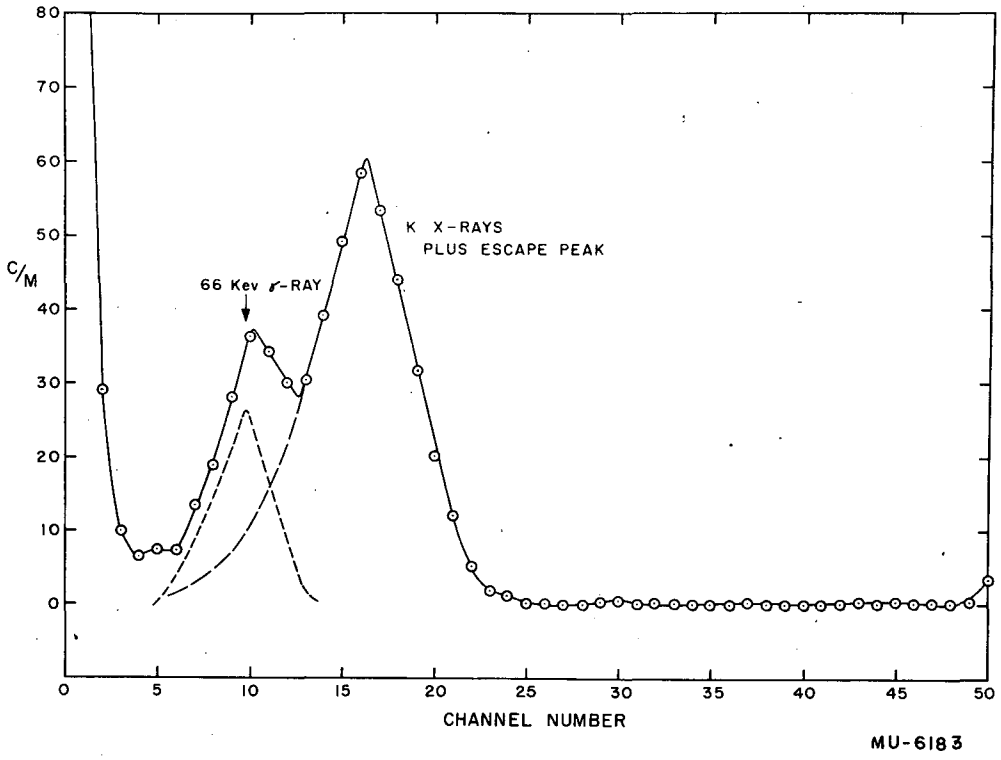

Fig. 9. Gamma ray spectrum of Np^{235}.

K x-rays : L x-rays : 66 Kev γ = 64 : 1000 : 16.

Using fluorescence yield values for K and L x-rays of uranium of 0.95 and 0.4 (see section D), a ratio of K to L shell vacancies of 27 : 1000 may be calculated. It is also necessary to correct for the L shell vacancies produced by filling of the K vacancies with L electrons (70 percent). Thus, K electron capture to L electron capture plus L conversion to 66 kev gamma ray ratios are calculated:

K capture : L capture + L conversion : 66 kev γ =

28 : 1000 : 7.

An examination of these ratios indicates that the 66 kev gamma ray could have an L conversion coefficient of approximately 80 as an upper limit with a corresponding K to L electron capture ratio of 0.06 as an upper limit. Theoretical calculations[37] predict conversion coefficients of 0.4, 24, and 125 for E1, M1, and E2 transitions, respectively, for a gamma ray of this energy. Thus, magnetic dipole or electric quadrupole radiation become probable assignments for the 66 kev transition.

The alpha decay of Pu^{239} yields some information on the level scheme of U^{235}. Three levels are populated by alpha decay, the two excited levels having 13 and 51 kev energy above the ground state. The occurrence of higher energy radiation in Pu^{239} is not in agreement with the observed alpha spectrum. Therefore, there is some doubt as to the ground state transition of Pu^{239} and a metastable state in U^{235} has been proposed.[43]

No radiation corresponding to the observed 66 kev gamma

ray has been found in Pu^{239} suggesting that the electron capture decay of Np^{235} is leading to a level in U^{235} not populated by alpha decay. Closed energy cycle relationships predict 0.170 Mev decay energy for electron capture of Np^{235}. The small K to L electron capture ratio is well-explained by noting that decay to a level at 66 kev in U^{235} can only be accomplished by L, M, etc. electron capture, the binding energy of a K electron (~116 kev) plus 66 kev amounting to more than the total decay energy available for electron capture. The small amount of K electron capture observed is probably due to a certain amount of branching decay to the ground state of U^{235}.

The spin of Np^{235} might be inferred as 5/2, analogous to the measured 5/2 spin of Np^{237}, [47] the 93rd proton being in an $f_{5/2}$ level. The spin of the ground state of U^{235} has been measured to be 5/2 [48] also, the 143rd neutron being in a $d_{5/2}$ level. It can be seen that electron capture decay to the ground state would involve no spin change but a change of parity. If the 66 kev gamma ray were an E1 transition, no parity change would occur in electron capture to this state, while M1 or E2 assignments for this gamma ray indicate a parity change for electron capture decay to the excited level.

F. Plutonium 234

Plutonium 234 was first discovered in the plutonium fraction separated from a bombardment of U^{233} with helium ions done by Hyde, et al. [41] The alpha particles of this isotope were reported to decay with an approximate 8-hour half-life. Later studies of

Pu^{234} by Perlman, et al.[49] and Orth[10] determined a best value of 9.0 hours for the half-life and an alpha to electron capture decay branching ratio of 1 to 25.

This isotope was produced for study in a similar bombardment of U^{233} with helium ions. A search was made for electromagnetic radiation resulting from the electron capture decay. No gamma rays were observed, the only features of the spectrum being the K and L x-rays of neptunium. An upper limit of 0.5 percent of the total disintegrations may be set for the abundance of a possible gamma ray. However, this does not preclude the existence of low energy radiation which is highly converted, particularly since no data have been obtained on the conversion electron spectrum. Orth[10] suggests the possible existence of appreciable low energy conversion electrons. It is probable, therefore, that the electron capture decay of Pu^{234} is proceeding directly to the ground state of Np^{234} although it is possible that a low energy excited state of Np^{234} is being populated and the radiation is not being observed. A decay energy of 0.21 Mev for the electron capture of Pu^{234} has been estimated by Seaborg, et al.[2] using closed decay cycles.

The spin of the ground state of Pu^{234} would be expected to be zero with even parity in line with other even-even nuclei while the prediction of the Mayer shell model for the daughter nucleus, Np^{234}, would be odd parity. A possible explanation of the data on the decay of Np^{234} (see section D) includes an assignment of a large spin value to the Np^{234} nucleus. These ideas suggest a large spin difference and a parity change in the electron capture decay of

Pu^{234} which, however, is not indicated by its comparative half-life from a correlation of ft values in section IV.

G. Plutonium 237

Plutonium 237, a 40-day electron capture isotope, was first reported by James, et al.[40] as a product from a bombardment of uranium with helium ions. Electromagnetic radiation identified as K and L x-rays of neptunium was the only radiation observed using absorption techniques. The alpha branching of Pu^{237} has not yet been established.

This isotope has been produced in a helium ion bombardment of U^{235} and in a proton bombardment of Np^{237}. The K and L x-rays of neptunium, products of the electron capture, have been observed to decay with a 40-day half-life using a sodium iodide crystal scintillation spectrometer and a xenon proportional counter. In addition to the x-rays, a 64 kev gamma ray has also been detected. The gamma ray spectrum as observed using the sodium iodide crystal spectrometer is shown in Figure 10. The dotted line indicates the K x-ray photoelectric peak plus the escape peak which amounts to about 15 percent of the photoelectric peak. This line was derived experimentally using an electron capture isotope which has no gamma rays in this region (Np^{234}). When the abundance and energy of the K x-ray peak of Np^{234} were normalized to the observed spectrum of Pu^{237} and subtracted from it, a gamma ray of approximately 64 kev energy was resolved. The electromagnetic radiation was calculated to be in the following relative abundances:

K x-rays : L x-rays : 64 kev γ = 100 : 77 : 39.

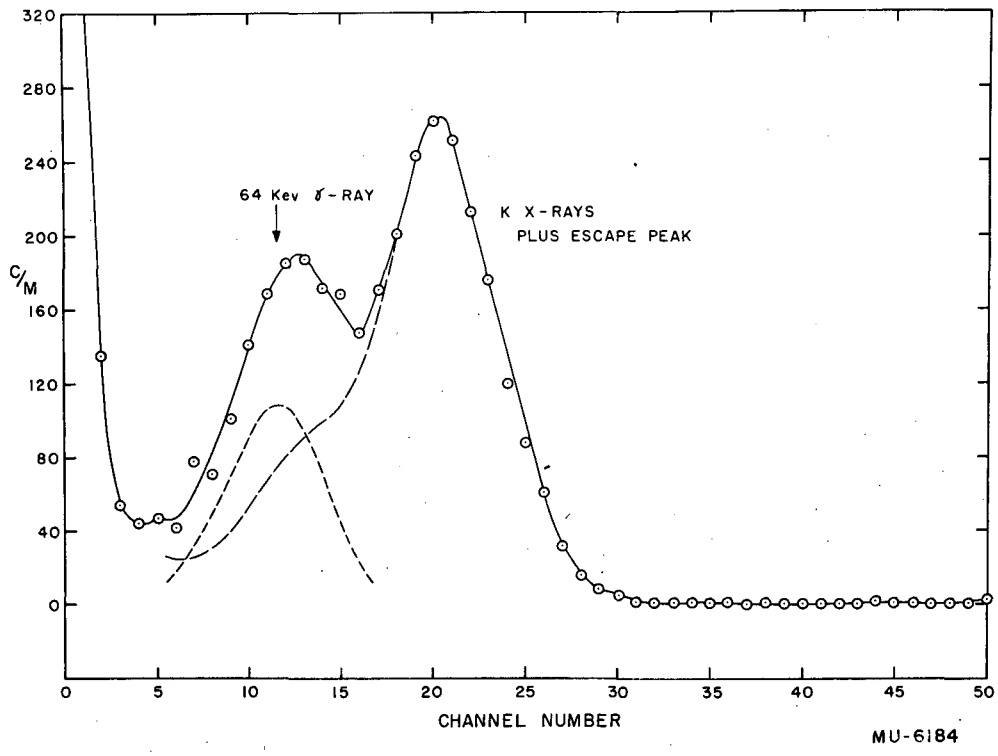

Fig. 10. Gamma ray spectrum of Pu^{237}.

The above value may be converted to a ratio of K to L shell vacancies when corrected using the appropriate fluorescence yield values. For the x-rays of neptunium, a fluorescence yield of 0.95 will be assumed, while for the L x-rays of neptunium an effective fluorescence yield of 0.4 is derived from the values reported by Kinsey. By again assuming that 70 percent of the K shell vacancies are filled by L electrons, K electron capture to L electron capture plus L conversion to 64 kev gamma ray ratios may be calculated:

K capture : L capture + L conversion : 64 kev γ =

105 : 119 : 39.

The 64 kev gamma ray is thought to be identical with the 60 kev transition observed in the alpha decay of Am^{241} [50] and the beta decay of U^{237}. [51] It is probable that the discrepancy in energy arises from the uncertainty in subtraction of the escape peak of the neptunium K x-rays (~102 kev) at approximately 73 kev from the observed spectrum. A portion of the level scheme for Np^{237} derived from alpha and beta decay data is presented in Figure 11. The presence of 60 kev radiation in both the alpha decay of Am^{241} and the beta decay of U^{237} suggests that this same level is populated by the electron capture decay of Pu^{237}. The evidence for a level 10.8 kev below that shown in Figure 11 as the ground state of Np^{237} from alpha decay data has been shown to be due to an instrumental effect rather than another alpha group. [52] Since the gamma ray seen in Pu^{237} decay is thought to be identical to that in Am^{241} decay, the conversion coefficient for this transition as observed by Beling, et al. [53] can be used to calculate a ratio of K to L electron

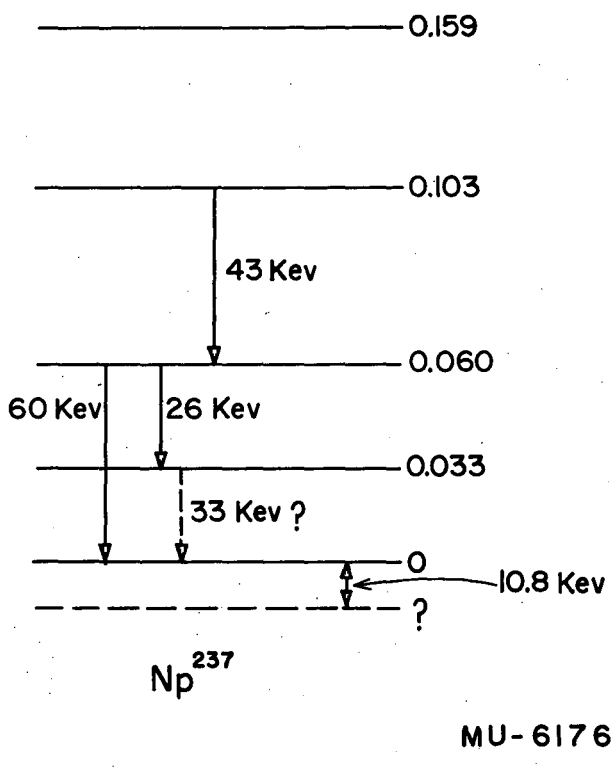

Fig. 11. Level scheme of Np^{237}.

capture. They report a value of 1.5 as an upper limit for the conversion coefficient of the 60 kev gamma ray. Assuming 75 percent of the total conversion coefficient is due to conversion in the L shell, i.e., the L conversion coefficient is equal to 1.1, the L x-rays arising from L conversion may be subtracted from the total L x-ray abundance observed. Likewise, the total conversion coefficient, 1.5, allows the calculation of the total 60 kev transitions from the observed abundance of the gamma ray. Thus, the following ratios have been calculated:

K capture : L capture : electron capture to 60 kev level =

100 : 67 : 93.

The above ratios indicate that approximately 56 percent of the electron capture of Pu^{237} proceeds to the 60 kev level in Np^{237}. Decay of the 60 kev level via the emission of 27 and 33 kev gamma rays in cascade would lower the value for the conversion coefficient of the 60 kev gamma ray which was calculated from the experimental ratio of 60 kev gamma rays observed per alpha particle in Am^{241} decay. However, the above corrections to the L x-ray abundances would not be affected since the 27 and 33 kev gamma rays would be expected to have large L conversion coefficients. The total decay energy available for electron capture is 0.22 Mev as estimated by Seaborg, et al.[2] in calculations from closed decay cycles. It can be seen that electron capture decay to the levels at 103 and 159 kev could be only L, M, etc. electron capture since K electron capture would be energetically impossible. The appreciable K electron capture branching of this isotope suggests that most of the electron

capture proceeds to the 60 kev level or lower levels of Np^{237}.

The ground state spin of Np^{237} has been measured to be 5/2, the 93rd proton being in an $f_{5/2}$ level, while the spin of Pu^{237} can be inferred from the spin of the 143rd neutron in U^{235}, measured to be 5/2, a $d_{5/2}$ level. The 60 kev gamma ray has been reported to be an E1 transition[53] from the experimental conversion coefficient and an M1 - E2 mixture[22] from the ratios of L vacancies and the L_I conversion coefficient. The data which lead to an E1 assignment for the 60 kev transition seem to involve fewer uncertainties than the latter work, although the measured lifetime[53] of this state does not agree with what is expected theoretically for an E1 transition. Thus, electron capture decay to the ground state would involve no spin change but a change of parity, while decay to the 60 kev level would involve a possible 0, ±1 change of spin and no change of parity assuming the gamma ray to be an E1 transition.

H. Americium 242m

The two isomers of Am^{242}, the 16-hour Am^{242m} and the long-lived (approximately 100 years) Am^{242}, the ground state, were first observed as neutron capture products of Am^{241}.[54-56] The decay characteristics of these isomers, particularly Am^{242m}, have been studied in detail by O'Kelley, et al.[57] The results of their investigation might best be summarized in a decay scheme shown in Figure 12.

A neutron irradiation of Am^{241} in the MTR reactor at Arco, Idaho, produced the Am^{242m} which was studied in the present

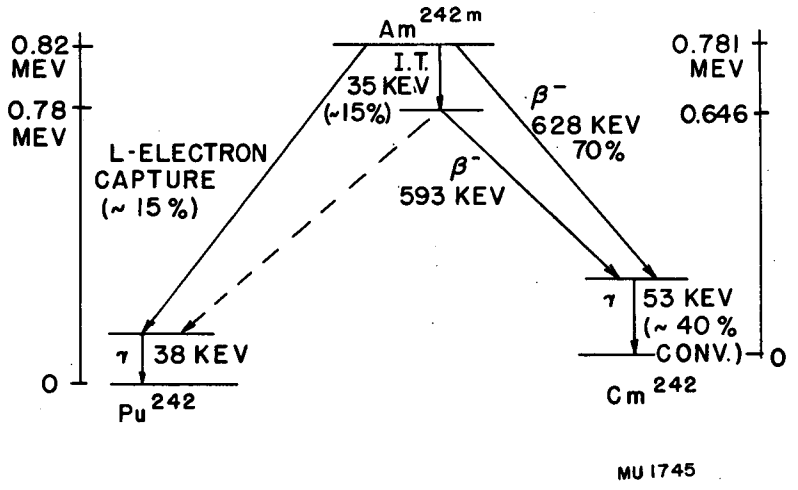

Fig. 12. Decay scheme of Am^{242} and Am^{242m} (O'Kelley).

investigation. A purified sample of irradiated americium consisting of about 1.5 milligrams total mass, was mounted in the bent crystal gamma ray spectrometer and the gamma spectrum examined in the 13-60 kev region. L x-ray lines of four elements were resolved, those of neptunium, plutonium, americium, and curium. In addition, three possible gamma rays were seen at 42.3, 43.6, and 44.8 kev. These were of extremely low intensity and therefore cannot be definitely considered real, although they were observed on both sides of the midpoint of the instrument. The L x-ray spectrum resembles that obtained by O'Kelley and co-workers and resolution of certain peaks not seen previously was allowed by the greater specific activity of our sample. A portion of this spectrum showing the L α lines of all four elements is shown in Figure 13. In particular, the americium and plutonium L_{α_2} lines were clearly seen, the plutonium L_{β_3} and americium L_{β_4} lines were observed together in one peak, and the neptunium L_{γ_1} line was also resolved. The origin of the L x-rays from the different elements might be considered here. The neptunium L x-rays most certainly arise from the conversion of gamma rays following the alpha decay of the Am^{241} as evidenced by the fact that no decay of the x-ray peaks is seen. The L x-rays of plutonium and curium are thought to arise from the conversion of gamma rays following electron capture and beta decay of the Am^{242m} and from the electron capture process itself, while the americium L x-rays are a result of the isomeric transition of Am^{242m} to the ground state. However, the origin of these americium x-rays might be

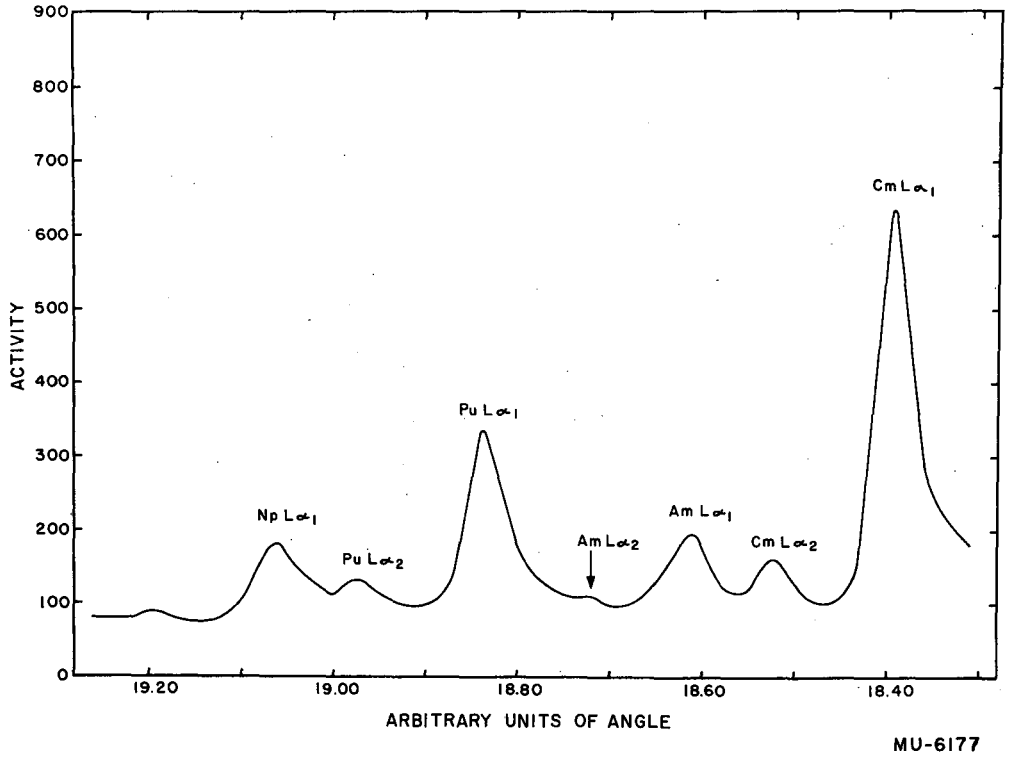

Fig. 13. L_α x-rays of Cm, Am, Pu, and Np.

considered doubtful in view of the fact that the americium L_{α_1} line still appeared after long decay. The presence of these americium x-rays might be explained, at least in part, by self excitation. In particular, the curium L_{β_1} line at 19.47 kev, is just above the americium L_{III} edge (at approximately 18.5 kev) which would suggest a large cross section for photoelectric absorption. The intensity of the curium L_{β_5} line, whose extrapolated energy (18.86 kev) coincides with that of the americium L_{β_1} line (18.80 kev), has been subtracted from the americium L_{β_1} intensity using the ratio of intensities of the L_{α_1} and L_{β_5} lines found in a previous experiment and the observed intensity of the L_{α_1} line in this sample. As a result, the intensity of the americium L_{β_1} x-ray was reduced by more than half, while much of the intensity of the americium L_{α_1} line may be due to photoelectric absorption of the curium L_{β_1} x-ray. These corrections cast serious doubt on the amount of decay occurring by isomeric transition in Am^{242m} and allow an upper limit of 5 percent to be set for branching decay by this method.

Certain of the calculated relative intensities of the various L x-rays differ from previous work mainly because improved corrections for absorption in the system and counting efficiency were used. From the various intensities of the lines, the relative number of vacancies have been calculated:

Transitions	Relative Intensities	
	Pu	Cm
ΣL_{II}	730	2500
ΣL_{III}	290	1110

These give the ratio of yields of curium to plutonium directly:

$$\left(\frac{Cm}{Pu}\right)_{L_{II}} = \frac{2500}{730} = 3.4$$

$$\left(\frac{Cm}{Pu}\right)_{L_{III}} = \frac{1110}{290} = 3.8.$$

The average of the above values, 3.6, is in fair agreement with a measured ratio of 4.2 for Cm^{242} to Pu^{242} formed during the neutron irradiation.[58] It was necessary to correct the plutonium x-ray intensities for the L x-rays arising directly from the electron capture process. The assumption was made that most of the electron capture occurred either in the K or L_I shells, the K x-rays leaving vacancies in some cases in the L_{II} and L_{III} shells and thus giving rise to some L_{II} and L_{III} x-rays. The observed L_{II} and L_{III} x-rays were then reduced by the calculated amounts. The intensity of the K x-rays was determined relative to the intensity of the 60 kev gamma ray of Am^{241} using a sodium iodide crystal spectrometer. The ratio of K to L electron capture then becomes 0.7, assuming all the electron capture is either K or L_I.

The conversion electron spectrum of Am^{242m} obtained using the beta ray spectrometer is shown in Figure 14. The resolution obtained on this sample is greater than before, probably due to the greater specific activity of the material allowing a sample of smaller mass to be used. A second difference noticeable in this spectrum, in contrast to that obtained in previous work,[57] is the lower relative abundance of the electron lines in the 0.340

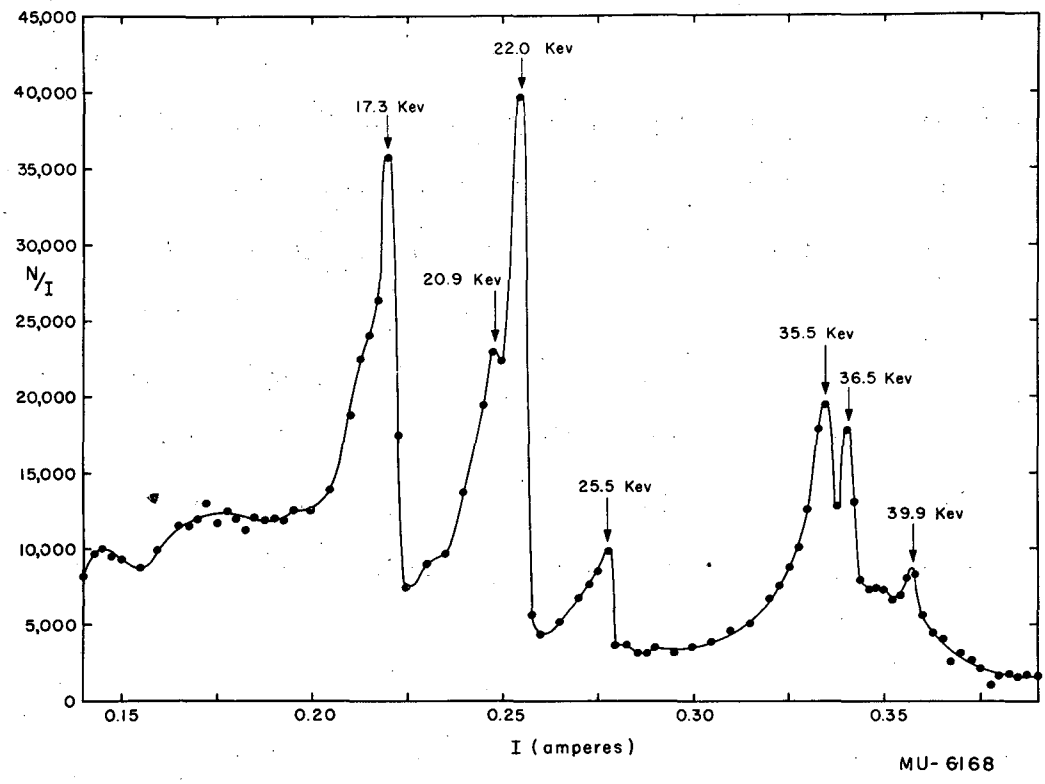

Fig. 14. Conversion electron spectrum of Am^{241m}.

ampere region. This fact may be explained by the use of a thinner window on the counter during these runs on the beta ray spectrometer. Data on the conversion electrons and corresponding gamma rays are shown in Table 2. The conversion electron peaks listed decayed with an approximate 16-hour half-life. The two most abundant peaks at 17.3 and 22.0 kev are assigned to the L conversion of a gamma ray in curium since the L x-rays of curium are most abundant and gamma rays in this energy region would be expected to be highly converted in the L shells. The electron lines at 35.5, 36.5, and 39.9 kev then fit well when assigned to M and N shell conversion. The gamma ray energy is best determined from the L_{II} and L_{III} conversion electrons to be 41.0 kev. The two remaining lines at 20.9 and 25.5 kev may be assigned to the L_{II} and L_{III} conversion of a 43.3 kev gamma ray in plutonium. The electron line at 39.9 kev might then conceivably be an M shell conversion of this 43.3 kev gamma ray, although the curium M conversion line is a better assignment energetically. The absolute uncertainty on the gamma ray energies is about ±2 kev.

Two of the gamma rays observed on the bent crystal spectrometer (42.3 and 44.8 kev) differ by 2.5 kev, which compares favorably with a 2.3 kev difference from the conversion electron data. The intensities of the two gamma rays indicate L conversion coefficients of >200 when compared with the L x-ray intensities. The L_{II} to L_{III} conversion ratios for plutonium and curium agree with the L_{II} to L_{III} x-ray ratios, although the intensities of curium L_{II} : plutonium L_{II} and curium L_{III} : plutonium L_{III} differ somewhat from the x-ray values. In light of

these new experimental data, a revised decay scheme is presented for Am^{242m} in Figure 15.

Table 2

Gamma Ray	Conversion Shell	Electron Energy	Relative Intensity
41.0 kev	Cm L_{II}	17.3 kev	100
	Cm L_{III}	22.0	74
	Cm M_{II}	35.5	67
	Cm M_{III} or M_{IV}	36.5	44
	Cm N (Pu M?)	39.9	22
43.3 kev	Pu L_{II}	20.9	59
	Pu L_{III}	25.5	23

The data obtained by O'Kelley on the beta spectrum of Am^{242m} have been confirmed in a determination made with the present sample. Thus the energy difference between the isomer and the ground state remains 35 kev if the beta minus decay of the Am^{242} ground state also proceeds to the first excited state of Cm^{242}. This is not necessarily the case, for the presence of an isomer indicates a considerable difference in spin so that beta decay to the same state would not be expected. It was not possible to determine if the same conversion electrons were present in Am^{242} ground state decay after the Am^{242m} had disappeared due to the presence of conversion electrons from 60 and 43 kev transitions in Am^{241}. However, Jaffe[59] has reported observation of 100 kev radiation with a sodium iodide scintillation spectrometer from a sample of long-lived

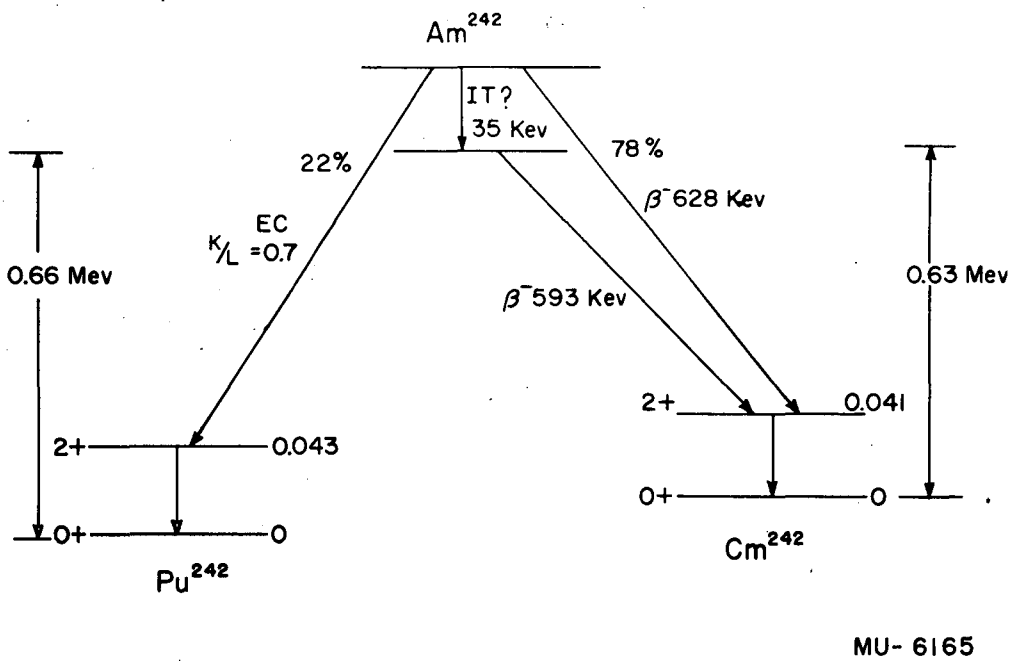

Fig. 15. Revised decay scheme for Am^{242m}.

Am^{242} which has been interpreted as K x-rays of plutonium indicating a branching of approximately 10 percent K electron capture for the ground state of Am^{242}.

The 41 kev spacing of the first excited level of Cm^{242} above the ground state is in good agreement with the results of Dunlavey and Seaborg[60] for the complex alpha structure of Cf^{246}. They found an excited level 43 kev above the ground state using nuclear emulsions to observe the L and M conversion electrons in coincidence with the Cf^{246} alpha particle. The ground states of Cm^{242} and Pu^{242} are assigned spin zero with even parity while the first excited levels in each isotope are assigned spin two with even parity in line with the expected spins and parities for even-even nuclides.[39] The 41 and 43 kev radiations are, therefore, E2 transitions. Rather large L conversion coefficients (>400) would be expected for electric quadrupole radiation of these energies according to theoretical calculations.[37]

Closed decay cycles predict an electron capture energy for Am^{242}, ground state, of 0.66 Mev. Thus, for Am^{242m}, a decay energy of 0.65 Mev is calculated for electron capture to the 2+ state. The electron capture and beta minus decay would be expected to be to levels of similar spin, for the decay energies and levels in Pu^{242} and Cm^{242} available for decay are much alike. A K to L electron capture ratio of 0.7 seems rather small for the amount of decay energy available. Electron capture branching from Am^{242m} to the ground state of Pu^{242} is not ruled out from these data. However, the lack of complexity of the beta minus spectrum of Am^{242m} suggests that, in parallel fashion, most of

the electron capture occurs to the first excited level.

IV. DISCUSSION OF RESULTS

In correlating experimental results with electron capture theory, it is first necessary to examine beta decay theory in general. The first detailed theory of the process was presented by Fermi.[61] He introduced a new interaction between the nucleon and the two light particles, the electron and the neutrino. This interaction was chosen in analogy with the spontaneous emission of light by atoms. Thus, although the electron and neutrino do not exist within the nucleus, it was proposed that they are emitted from the nucleus as a result of an interaction between the nucleons and the electron-neutrino field.

The theories of beta decay that have been developed since Fermi are logical developments according to the perturbation theory of quantum mechanics, if one has assumed a certain form for the interaction Hamiltonian. All theories are based on the neutrino hypothesis and the Dirac equation for nucleons and leptons (electrons and neutrinos). The interactions that may be assumed are only restricted by the conditions of relativistic invariance. According to the Dirac theory five independent relativistically invariant expressions can be chosen for the interaction Hamiltonian,[62] which are usually called the scalar, vector, tensor, axial vector, and pseudoscalar interaction. Taking one of these forms singly is the natural generalization of Fermi's original choice, which was the polar vector form. This choice was dictated by the analogy of the electromagnetic field. Linear

combinations of these five invariants can also be chosen.[63]

The Fermi theory of beta decay imposes the selection rule $\Delta I = 0$ (I = total angular momentum of the nucleus) arising from the orthogonality of the nuclear wave functions for states of different angular momentum. There is good evidence, however, that this selection rule is not generally adhered to. In particular, the large probabilities for the beta decay of He^6 and the electron capture of Be^7 violate this rule in that each transition involves a spin change of one unit. Gamow and Teller[64] introduced a modification to Fermi's theory according to which an "allowed" transition may involve a spin change of zero or one unit of angular momentum. The interactions which allow a spin change of one are the tensor and axial vector forms. The other three may be called Fermi type interactions while these two are called Gamow-Teller type interactions.

In general, the probability for beta decay may be written in the following form:

$$d\lambda = \left(\frac{2\pi}{\hbar}\right) \left| \int \psi^*_{fin.} \, H\psi_{in.} \, d\tau \right|^2 \cdot \rho(E)dE,$$

where H = Hamiltonian of the interaction between the proton, neutron, and electron-neutrino fields,

$\rho(E)$ = the number of final states of the system per unit energy interval,

$\psi_{in.}$ = wave function of initial state of the system,

$\psi_{fin.}$ = wave function of final state of system.

Marshak[65] has used the tensor interaction to find a general formula for probability of allowed and forbidden electron capture. To

determine the probability for K electron capture the wave function for an electron bound in the K shell is used instead of a wave function for a free electron with one of a spectrum of energies. Using relativistic wave functions for the atomic electrons, the density of an s electron at the nucleus for an unscreened hydrogen-like atom may be calculated. Marshak gives expressions for the large and small components of the Dirac wave functions for K, L_I, L_{II}, and L_{III} electrons at the nucleus. Approximate allowance for screening is made in these equations by replacing Z by an effective charge, i.e., $Z_K = Z-0.30$ and $Z_L = Z-4.15$.[66] More accurate electron wave functions, namely relativistic wave functions for a Thomas-Fermi atom with exchange, have been calculated by J. Reitz[67] on the ENIAC. As a check, the K and L_I electron densities at the edge of the nucleus were calculated for uranium using these more accurate wave functions and were compared to densities derived from the equations given by Marshak. The results were found to agree within a few percent, and, therefore, it was felt that the equations given by Marshak are accurate enough for our purpose.

Upon substituting the proper quantities into the general equation for beta decay, the probability for allowed electron capture becomes:

$$d\lambda = \left(\frac{G^2}{2\pi^3}\right) |M|^2 \left(\frac{\pi}{2}\right) [\ (W_o + W_K)^2\, n_K g_K^2 + (W_o + W_L)^2\, n_{L_I} g_{L_I}^2 +$$

$$(W_o + W_L)^2\, n_{L_{II}} f_{L_{II}}^2\ ]\ dW,$$

where $G^2/2\pi^3$ = a constant indicating strength of coupling between nucleon and electron-neutrino fields,

M = matrix element; contains wave functions of initial and final states of nucleon and interaction Hamiltonian,

W_o = disintegration energy/mc^2 - 1,

$W_{K, L}$ = binding energy of orbital electron,

n_{K, L_I}, etc. = number of electrons in shell,

g_{K, L_I} = large component of Dirac wave function,

$f_{L_{II}}$ = small component of Dirac wave function.

In an allowed transition for the tensor interaction, only an s electron will be captured with any appreciable probability. Thus, K and L_I capture will compete under favorable circumstances. In an allowed transition, there will be a small probability for L_{II} capture due to the small component of the $p_{1/2}$ Dirac wave function which has s character. The maximum allowable spin change is one unit of angular momentum for an allowed transition. For a first forbidden transition, p electrons will also be captured along with s electrons; a nuclear spin change of two units is permitted in a first forbidden transition.

For electron capture it is not necessary to integrate the above equation over a spectrum of energies since the neutrino is emitted with a discrete energy. Hence, we may write for allowed electron capture:

$$\lambda_{EC} = \left(\frac{G^2}{2\pi^3}\right) |M|^2 f_{EC},$$

where $f_{EC} = \frac{\pi}{2} [(W_o + W_K)^2 n_K g_K^2 + (W_o + W_L)^2 n_{L_I} g_{L_I}^2 +$

$$(W_o + W_L)^2 n_{L_{II}} f_{L_{II}}^2].$$

By rearranging, it can be shown that

$$(ft)_{EC} = \ln 2 \left(\frac{2\pi^3}{G^2}\right) \frac{1}{|M|^2},$$

where t = partial half-life for electron capture.

It is now obvious that the product ft should be independent of energy release and nuclear charge for allowed transitions. If the lowest order terms in the expansion of the electron and neutrino waves give a zero matrix element in accordance with selection rules, the transition is termed forbidden. However, a contribution is still possible from higher order terms in the expansion and from the "small" relativistic terms which had been neglected. Hence, it becomes possible to determine the degree of forbiddenness of a transition from its ft value; the larger ft values denoting more forbidden transitions.[68] If the spin of the initial nucleus is less than the spin of the level to which the decay occurs, the ft value must be multiplied by a statistical factor, $(2I_f + 1)/(2I_i + 1)$. Unless the spins are known, it becomes difficult to apply this correction. Except in the case of large spin changes it will not result in an appreciable increase of the ft value.

The Gamow-Teller selection rules group beta transitions according to the following scheme:

Allowed: $\Delta I = 0, 1$ No parity change, No $0 \rightarrow 0$.

First forbidden: $\Delta I = 0, 1, 2$ Yes.

Second forbidden: $\Delta I = 2, 3$ No.

A further grouping of beta transitions according to spin and parity changes has been made in a study of nuclear shell structure and beta decay, the ft values falling within definite limits for various types of decay as listed in the following table:[69]

Spin Change	Parity Change	G-T Classification	log ft Odd A	log ft Even A
$\Delta I = 0, 1$	No	Allowed	4.5-5.9	4.1-5.7
$\Delta I = 0, 1$	Yes	First forbidden	6.0-7.8	5.5-7.8
$\Delta I = 2$	Yes	First forbidden	7.1-9.8	7.4-9.6
		$\log (W_o^2 - 1)$ ft	8.6-10.7	8.5-10.4
$\Delta I = 1$	No $\Delta \ell = 2$ (ℓ-forbidden)		4.9-7.0	5.9-9.0
$\Delta I \geq 2$	No	Second and higher forbidden	12.2-23.2	13.5-17.6

The $\Delta I = 2$ Yes group was identified by the unique shape for the beta spectra. Since the f factors for such transitions should be different from that of allowed transitions approximately by a factor $(W^2 - 1)$, the $\log (W_o^2 - 1)$ft has also been tabulated for this type of transition. A new group of transitions for which $\Delta I = 1$ No $\Delta \ell = 2$ was defined as ℓ-forbidden from a consideration of nuclear shell structure.

A calculation of the f_{EC} values has been made using the above mentioned formula for allowed electron capture for Z = 80, 90, and 100. A plot of f_{EC} values versus W_o is shown in Figure 16. In

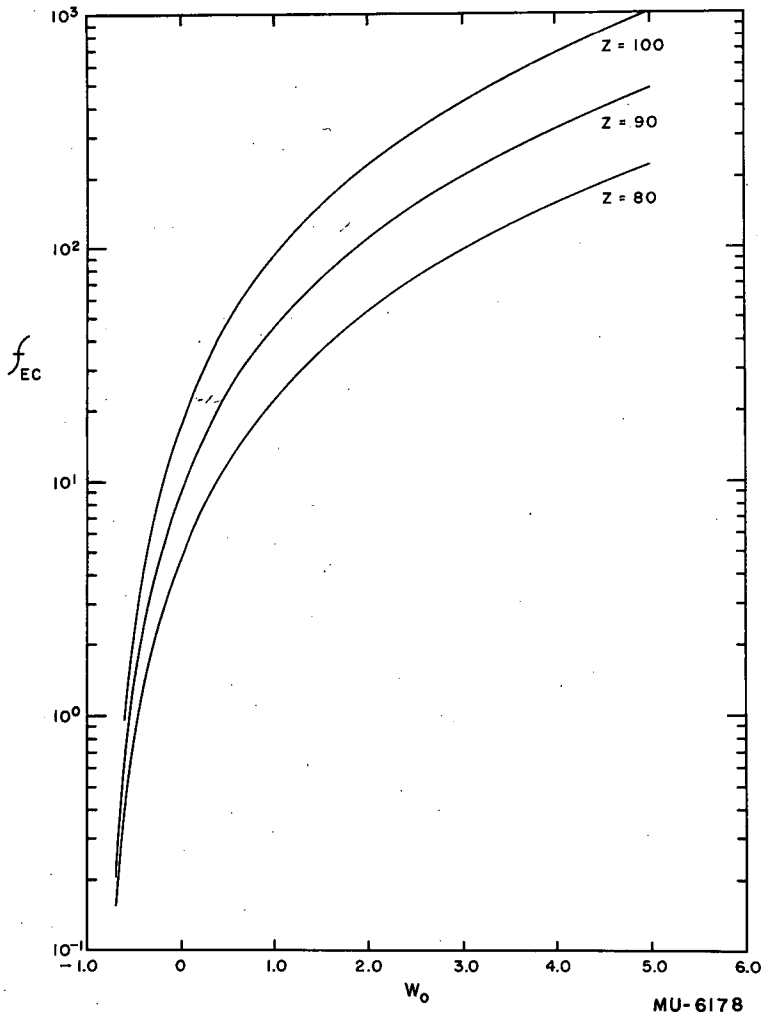

Fig. 16. Logarithm of f_{EC} as a function of W_o.

addition, K/L electron capture ratios similar to those calculated by Rose and Jackson[70] for allowed, first, and second forbidden electron capture have been calculated using the formulas given by Marshak. The results are shown in Figures 17, 18, and 19. Since the formulas for the probabilities of forbidden electron capture given by Marshak are only for the parity favored transitions, the calculated K/L electron capture ratios for forbidden electron capture may only apply to these parity favored transitions, namely first forbidden $\Delta I = 2$ Yes and second forbidden $\Delta I = 3$ No. For first forbidden decay where $\Delta I = 0, 1$ Yes and second forbidden decay where $\Delta I = 2$ No, i.e., parity unfavored transitions, other matrix elements can contribute and the K/L electron capture ratio may depend upon the relative size of the matrix elements.

Calculation of ft values for electron capture isotopes of the heaviest elements have been made where the following information was available: (1) electron capture partial half-life, (2) decay energy from closed decay cycles, and (3) possible decay scheme (not always available). The correlation of spin and parity assignments from the ft values with the experimentally studied nuclides is quite satisfactory.

For the decay of At^{211}, log ft was calculated to be 6.1. Since this is thought to be wholly a ground state transition, a $\Delta I = 0, 1$ Yes assignment is in good agreement with the prediction of a parity change by the nuclear shell model. The measured K/L electron capture ratio of approximately 7 may be compared with theoretical values of 6.0, 4.5, and 2.6 calculated for allowed, first,

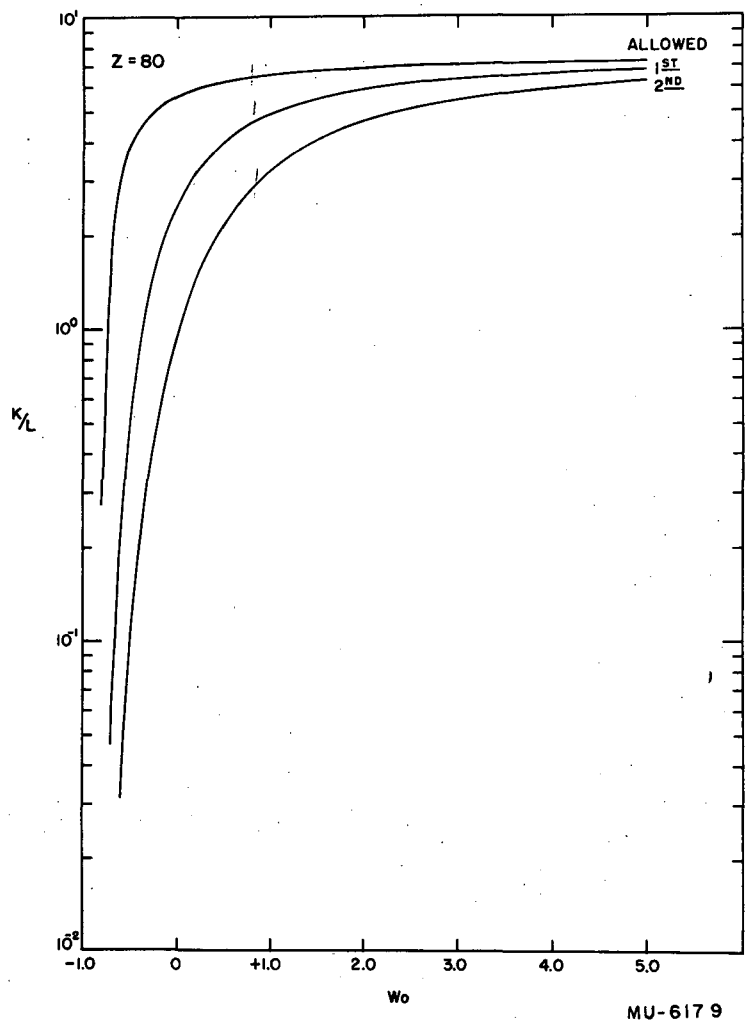

Fig. 17. Logarithm of K/L electron capture ratio as a function of W_o for Z = 80.

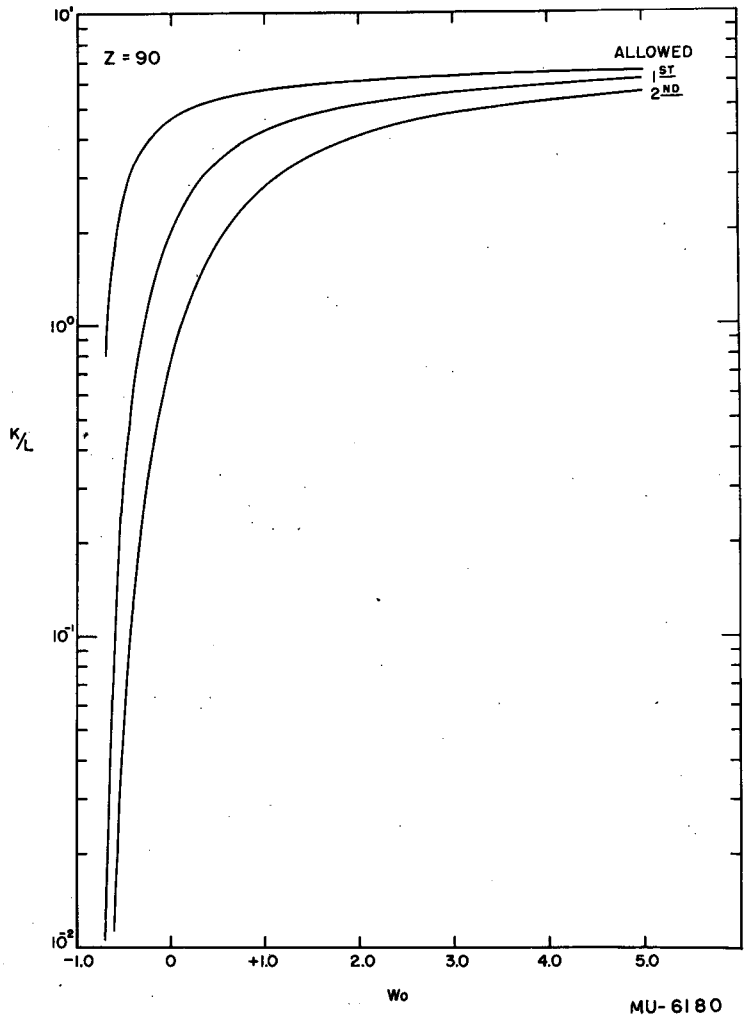

Fig. 18. Logarithm of K/L electron capture ratio as a function of W_o for Z = 90.

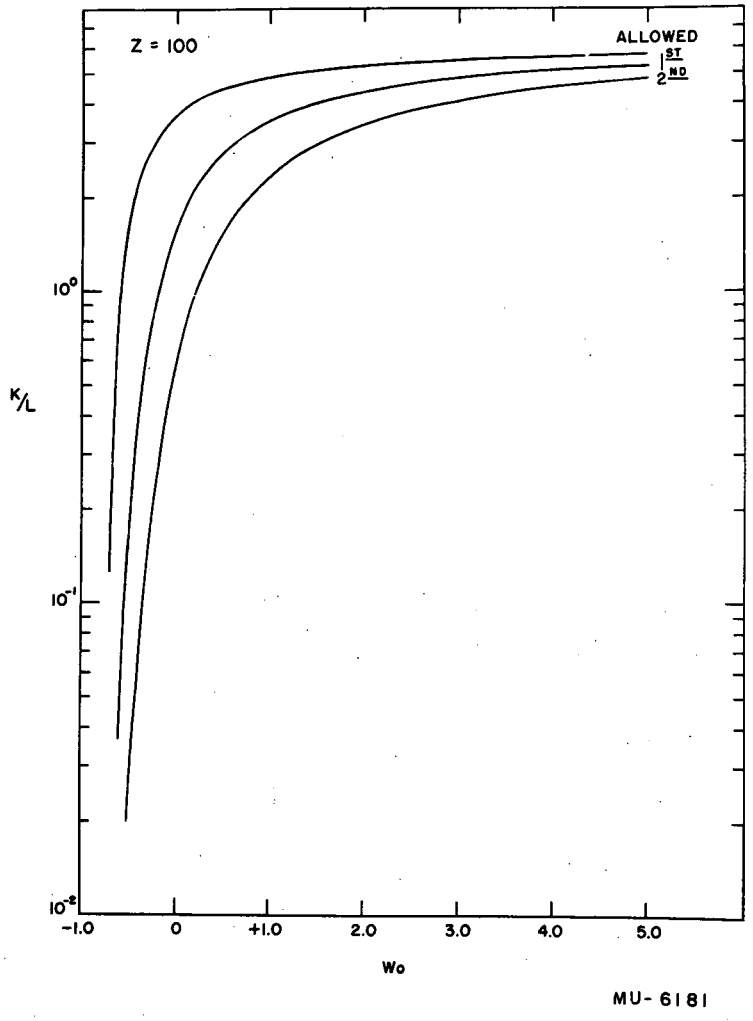

Fig. 19. Logarithm of K/L electron capture ratio as a function of W_o for Z = 100.

and second forbidden electron capture. The measured value seems to indicate an allowed transition which, however, is not predicted in its ft value.

The log ft values for the decay chain, $Pu^{234} \xrightarrow{\log ft = 5.5} Np^{234} \xrightarrow{\log ft = 5.6} U^{234}$, indicate $\Delta I = 0,1$ No (allowed) transitions for both Pu^{234} and Np^{234}. The allowed decay and the zero spin with even parity of the even-even nucleus, Pu^{234}, suggest electron capture decay to a 1+ level in Np^{234}, probably very near the ground state. The nuclear shell model predicts odd parity for the ground state of Np^{234} which indicates an odd parity assignment of the level at 1.57 Mev in U^{234}, the level being populated by the majority of the electron capture decay of Np^{234}. Theoretical K/L electron capture ratios of 2.1, 0.2, and 0.03 can be calculated for allowed, first forbidden, and second forbidden decay of Np^{234}, respectively. The experimental value, 1.0, falls between the predicted allowed and first forbidden values.

In the case of Np^{235}, all of the electron capture decay was assumed to proceed to a 66 kev level in U^{235}, the log ft for this decay equaling 6.3 which indicates $\Delta I = 0,1$ Yes for the transition. However, the measured spin of 5/2 with even parity assignment from the shell model for U^{235} and the inferred spin of 5/2 with odd parity for Np^{235} suggest electron capture branching to the ground state, also first forbidden.

The decay of Pu^{237} splits in approximately equal amounts between the ground state and the 60 kev level of Np^{237}. The log ft for the ground state transition is 6.8, a $\Delta I = 0,1$ Yes type of

transition in good agreement with the inferred spin of 5/2 with even parity for Pu^{237} and the measured spin of 5/2 with odd parity for Np^{237}. For the decay to the 60 kev level, a log ft of 6.3 was calculated indicating $\Delta I = 0, 1$ Yes. Since the 60 kev gamma ray is thought to be an E1 transition, the log ft might be considered too large and the decay to be allowed. The measured K/L electron capture ratio, 1.5, can be compared with theoretical ratios 1.5 and 0.6 calculated for first forbidden decay to the two levels.

Am^{242m} decays by both electron capture and beta minus decay to the first excited states (2+) of Pu^{242} and Cm^{242}, respectively. The log ft values for the decays are 6.7 and 6.9, both being $\Delta I = 0, 1$ Yes transitions. The straight-line Fermi plot for the beta minus decay agrees with this assignment. The possible spins for Am^{242m} are 1, 2, or 3 with odd parity. The experimental K/L electron capture ratio of 0.7 is in poor agreement with the theoretical ratio of 2.5 for first forbidden decay. The theoretical allowed K/L electron capture ratio is 4.5 while a second forbidden decay would have a theoretical K/L electron capture ratio of 1.2.

In general, the measured K/L electron capture ratios show agreement with theory. The ratio for At^{211}, approximately 7, is somewhat high for a first forbidden transition but the uncertainty in the determination becomes greater for larger K/L electron capture ratios. The K/L electron capture ratio of Am^{242m} is far below the predicted values and suggests further study of the measured value and calculated decay energy is necessary. As

already mentioned, caution must be used when comparing these experimental ratios with the calculated theoretical values.

In addition to those nuclides studied experimentally, there are a number of isotopes where electron capture to an excited level can be inferred, either from gamma rays observed in their decay or from the beta minus decay of an isotope to the same daughter nucleus. These nuclides are listed in Table 3.

A final group of nuclides exists for which decay schemes are not known. Log ft values have been calculated for these isotopes assuming ground state transitions, allowing them to be grouped according to types of transition in Table 4.

None of the above mentioned nuclei has been classified as ℓ-forbidden since the log ft limits for this type of transition are quite broad and knowledge of exact orbital assignments are lacking for the heaviest elements. It is also noted that most of the nuclides studied can be classified as either allowed or first forbidden, $\Delta I = 0, 1$ Yes. Two exceptions are Am^{240} and Cm^{241} which have log ft values large enough to allow assignment of $\Delta I = 2$ Yes. Analogous to the correlation of beta minus transitions of this type, the log ft value has also been calculated using an $f_{(1)}$ factor for a first forbidden transition, $\Delta I = 2$ Yes. These values, tabulated in Table 4, show near agreement with the limits for this type of transition in beta minus decay. This $f_{(1)}t$ value would be expected to be smaller for the heavier elements since it is dependent upon the square of the nuclear radius. The apparent lack of highly forbidden transitions is not surprising, in that the precise amount of electron capture branching to various excited levels is often

Table 3

Isotopes for which decay schemes can be inferred from beta decay data or from observed gamma rays:

Isotope	Total energy from closed cycles	Level[a]	Decay Energy	log ft	ΔI Parity
Bk^{245}	0.700	0.245 (γ-ray observed)	0.455	6.7	ΔI = 0,1 Yes
Am^{238}	2.22	1.03 (decay of Np^{238})	1.19	5.9	ΔI = 0,1 Yes
Am^{239}	0.780	0.277 (γ-ray observed, decay of Np^{239})	0.50	5.7	ΔI = 0,1 No
Np^{232}	2.65	1.05 (hard γ observed, decay of Pa^{232})	1.60	5.1	ΔI = 0,1 No
Np^{233}	1.09	0.30 (conv. e's observed, decay of Pa^{233})	0.79	4.8	ΔI = 0,1 No
U^{231}	0.34	ground state (50%)	0.34	6.4	ΔI = 0,1 Yes
	0.34	0.23 (50%) (decay of Th^{231})	0.11	4.7	ΔI = 0,1 No
Pa^{228}	2.05	1.03 (decay of Ac^{228})	1.02	6.6	ΔI = 0,1 Yes
Pa^{230}	1.28	0.94 (γ-ray observed)	0.34	6.7	ΔI = 0,1 Yes

[a]Data on levels has been taken from Table of Isotopes[44] with the exception of Bk^{245}.[15]

Table 4

Isotopes for which decay schemes are not known:

$\Delta I = 0, 1$ No			$\Delta I = 0, 1$ Yes			$\Delta I = 2$ Yes		
	Decay Energy	log ft		Decay Energy	log ft		Decay Energy	log ft
Am^{237}	1.48	5.9	Bk^{243}	1.46	6.5	(Am^{240}	1.53	7.5)
Pu^{232}	0.99	5.1	Bk^{244}	2.26	6.9	Cm^{241}	0.87	8.2
Pu^{235}	1.14	5.1	Cm^{238}	1.13	6.0			$\log f_{(1)}t$
U^{228}	0.30	3.8	Cm^{239}	1.79	6.4	Am^{240}	1.53	8.4
U^{229}	1.29	5.6	Am^{240}	1.53	7.5	Cm^{241}	0.87	8.5
Pa^{227}	1.08	5.9	Np^{236}	1.02	6.8			
Pa^{229}	0.37	5.8	Ac^{224}	1.37	6.0			
Th^{225}	0.55	4.7						
Ac^{223}	0.64	5.3						

very difficult to determine and the more highly forbidden transitions would be masked by the more predominant allowed decay. The small log ft, 3.8, for U^{228} is definitely low, even for allowed transitions in this region, and is thought to arise from a discrepancy in the calculated decay energy from closed decay cycles. An increase of 80 kev in the decay energy of U^{228} would place its log ft value within the limits for allowed electron capture.

The isotopes whose electron capture decay has been classified as allowed may decay to excited levels of daughter nuclei. In all cases for this region the odd proton and odd neutron will be in shells of different parity, according to the nuclear shell model. Thus all even Z nuclei would have even parity and all odd Z nuclei would have odd parity for Z = 89 → 97 and N (neutron number) = 134 → 148. Ground state transitions will involve parity changes and, therefore, allowed transitions would be expected to populate excited levels of daughter nuclei. In this region, many odd-odd nuclei are seen to decay to highly excited levels in the even-even daughter nucleus. For example, Np^{234}, Np^{238}, Pa^{232}, Pa^{234}, Ac^{228}, and others decay to levels at least one Mev above the ground state of the daughter nucleus. Therefore, it may be expected that similar decay will be observed when enough decay energy is available in certain odd-odd nuclei for which no experimental data are available (see Table 4).

A plot of the logarithm of the partial electron capture half-life versus the logarithm of the neutrino energy for allowed species is shown in Figure 20. This type of plot may be used with confidence, for the variation of electron capture probability with Z in this limited

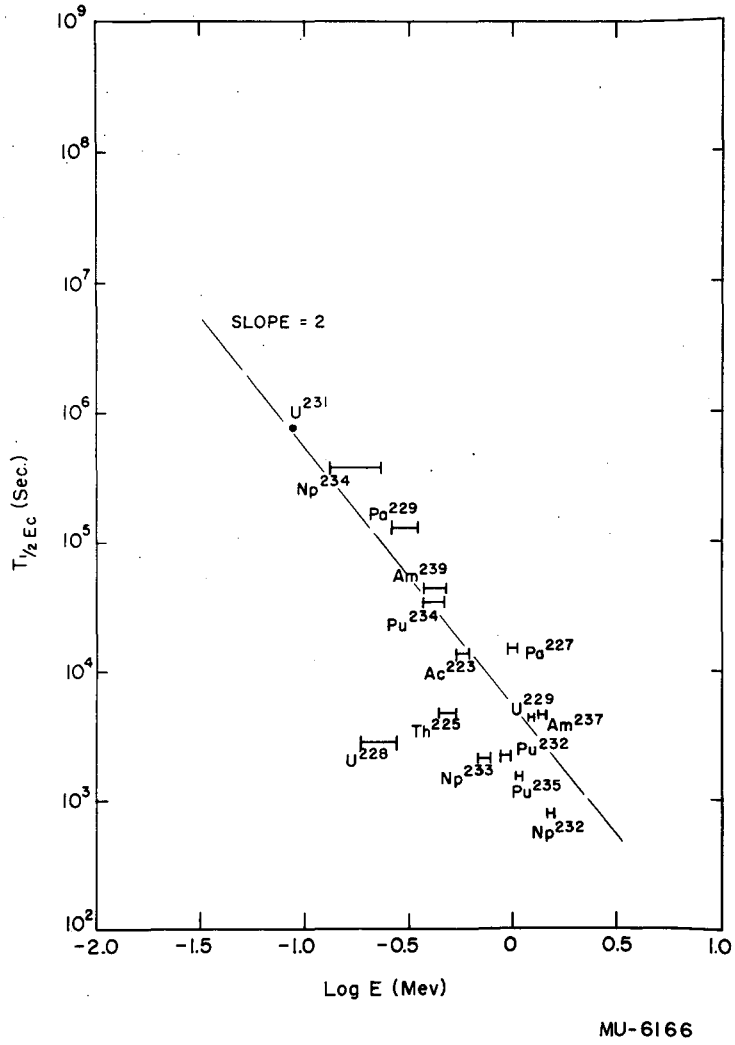

Fig. 20. Logarithmic plot of partial electron capture half-life versus neutrino energy for allowed species.

range is not great. The limits on the neutrino energy for each nuclide indicate K and L electron capture energies, the average decay energy lying somewhere between the limits depending on K to L electron capture ratio. The point for U^{231} decay to the excited level indicates only L, M, etc. electron capture is energetically possible. The theoretical expression for allowed electron capture predicts a slope of two for such a plot, i.e., the half-life depends upon the square of the neutrino energy. A line has been drawn, not as a best fit to the data, but as a reference line with the predicted slope. The data seem to fit a slope of approximately two, perhaps slightly greater. The nuclide, U^{228}, is again irregular, suggesting that the estimated decay energy is too small.

A similar plot for the first forbidden electron capture isotopes is shown in Figure 21. The point for Np^{235} indicates that only L, M, etc. electron capture is possible. For first forbidden decay, the theoretical expression[65] predicts a fourth-power dependence of half-life on neutrino energy. A reference line with a slope of four has been drawn. The data indicate a slope slightly less than four although greater than that of the allowed species. Curium 241 with a $\Delta I = 2$, Yes assignment falls well away from the rest of the nuclides. Certain other nuclides, all odd-odd nuclei, have points farthest from the majority of the data. As already mentioned, experimental examination may indicate a decay to excited levels which would cause these species to fall into line. It is expected that refinement of experimental data will lead to a verification of the predicted fourth-power dependence of half-life on energy.

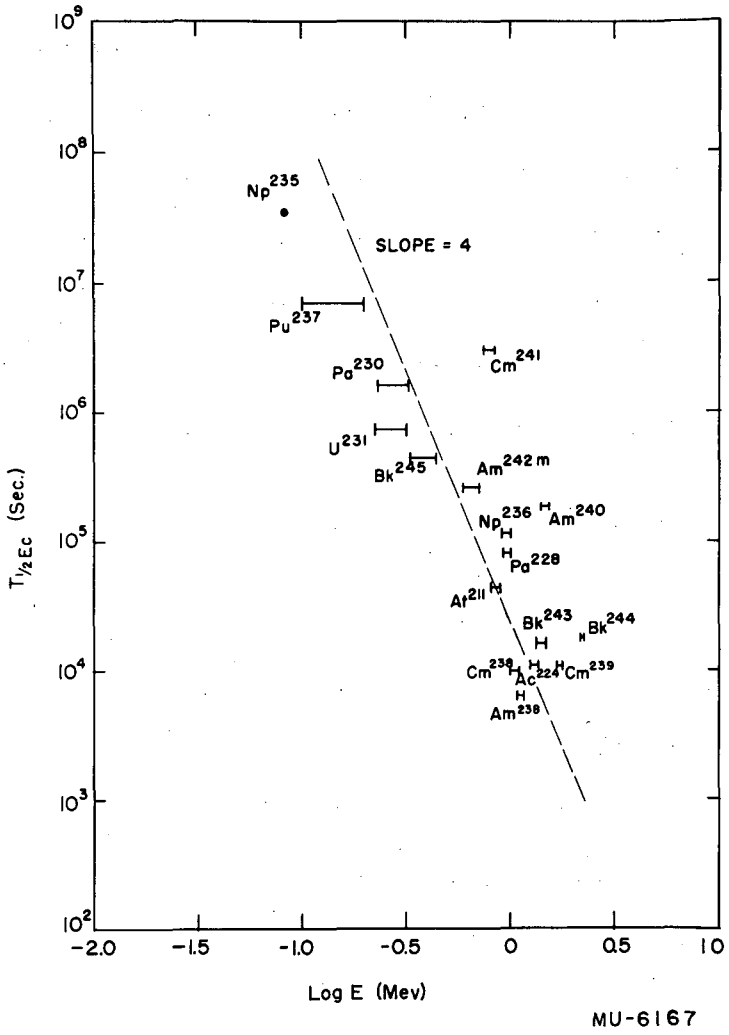

Fig. 41. Logarithmic plot of partial electron capture half-life versus neutrino energy for first forbidden species.

V. ACKNOWLEDGMENTS

The continued interest and helpful suggestions of Professor G. T. Seaborg throughout this investigation are gratefully acknowledged. The author wishes to express appreciation to Dr. S. G. Thompson whose continued guidance and assistance stimulated the progress of this research. Discussions with Dr. J. O. Rasmussen, Jr., have been most helpful, particularly with regard to electron capture decay theory.

The assistance of A. Ghiorso and A. E. Larsh, Jr. in the construction and maintenance of some of the instruments used in this investigation is greatly appreciated. Thanks are also due to the California Research and Development Company staff for the use of their counting equipment. The helpful discussions and assistance of Dr. F. Asaro, Dr. E. K. Hulet, T. O. Passel, and H. Jaffe are gratefully acknowledged. The author wishes to thank Miss H. Jensen for her computations involving electron capture decay theory.

The author also gratefully acknowledges the cooperation of Dr. J. G. Hamilton, G. B. Rossi, W. B. Jones, and the staff of the 60-inch cyclotron and the staff of the MTR reactor at the Reactor Testing Station, Arco, Idaho.

This work was performed under the auspices of the United States Atomic Energy Commission.

VI. LIST OF ILLUSTRATIONS

List of illustrations (cont'd) Page

VII. REFERENCES

1. I. Perlman, A. Ghiorso, and G. T. Seaborg, Phys. Rev. 77, 26 (1950).
2. G. T. Seaborg, R. A. Glass, and S. G. Thompson, to be published.
3. D. Maeder and P. Preiswerk, Phys. Rev. 84, 595 (1951).
4. S. G. Thompson, Phys. Rev. 76, 319 (1949).
5. N. Feather, Proc. Roy. Soc. (Edinburgh) 63A, 242 (1952).
6. M. G. Mayer, Phys. Rev. 75, 1969 (1949).
7. O. Haxel, J. H. D. Jensen, and H. E. Suess, Phys. Rev. 75, 1766 (1949).
8. E. L. Kelly and E. Segrè, Phys. Rev. 75, 999 (1949).
9. S. G. Thompson, A. Ghiorso, and G. T. Seaborg, Phys. Rev. 80, 781 (1950).
10. D. A. Orth, Ph. D. Thesis, University of California Radiation Laboratory Declassified Report UCRL-1059 Rev. (December, 1950).
11. D. R. Corson, K. R. MacKenzie, and E. Segrè, Phys. Rev. 57, 459, 1087 (1940).
12. G. L. Johnson, R. F. Leininger, and E. Segrè, J. Chem. Phys. 17, 1 (1949).
13. G. W. Barton, Jr., A. Ghiorso, and I. Perlman, Phys. Rev. 82, 13 (1951).
14. L. B. Asprey, S. E. Stephanou, and R. A. Penneman, J. Am. Chem. Soc. 72, 1425 (1950).
15. E. K. Hulet, Ph. D. Thesis, University of California Radiation Laboratory Unclassified Report UCRL-2283 (July, 1953).

16. A. Ghiorso, A. H. Jaffey, H. P. Robinson, and B. B. Weissbourd, National Nuclear Energy Series, Plutonium Project Record, The Transuranium Elements: Research Papers (McGraw-Hill Book Co., Inc., New York, 1949), Vol. 14B, 1226 (1949).

17. F. L. Reynolds, Rev. Sci. Inst. 22, 749 (1951).

18. A. Ghiorso and A. E. Larsh, Jr., to be published.

19. P. M. McLaughlin and G. D. O'Kelley, California Research and Development Company Report, MTA-40 (1953).

20. G. D. O'Kelley, Ph. D. Thesis, University of California Radiation Laboratory Unclassified Report UCRL-1243 (May, 1951).

21. G. W. Barton, Jr., H. P. Robinson, and I. Perlman, Phys. Rev. 81, 208 (1951).

22. C. I. Browne, Jr., Ph. D. Thesis, University of California Radiation Laboratory Unclassified Report UCRL-1764 (June, 1952).

23. H. M. Neumann and I. Perlman, Phys. Rev. 81, 958 (1951).

24. D. R. Corson, K. R. MacKenzie, and E. Segrè, Phys. Rev. 58, 672 (1940).

25. R. F. Leininger, E. Segrè, and F. N. Spiess, Phys. Rev. 82, 334 (1951) (A).

26. L. S. Germain, Phys. Rev. 78, 90 (1950).

27. H. Küstner and E. Arends, Ann. Physik 22, 443 (1935).

28. B. B. Kinsey, Can. Journal of Res., 26A, 404 (1948).

29. C. D. Broyles, D. A. Thomas, and S. K. Haynes, Phys. Rev. 89, 715 (1953).

30. R. M. Steffen, O. Huber, and F. Humbel, Helv. Phys. Acta 22, 167 (1949).

31. C. D. Ellis, Proc. Roy. Soc. A139, 336 (1933).

32. A. Flammersfeld, Z. Physik 114, 227 (1939).

33. F. F. Momyer, Ph. D. Thesis, University of California Radiation Laboratory Unclassified Report UCRL-2060 (February, 1953).

34. D. H. Templeton, A. Ghiorso, and I. Perlman, unpublished data (June, 1948).

35. H. M. Neumann, A. Ghiorso, and I. Perlman, unpublished data (1950).

36. M. Goldhaber and A. Sunyar, Phys. Rev. 83, 906 (1951).

37. H. Gellman, B. A. Griffith, and J. P. Stanley, Phys. Rev. 85, 944 (1952).

38. M. E. Rose, G. H. Goertzel, and C. L. Perry, Oak Ridge National Laboratory Unclassified Report ORNL-1023 (June, 1951).

39. G. Scharff-Goldhaber, Phys. Rev. 90, 587 (1953).

40. R. A. James, A. E. Florin, H. H. Hopkins, Jr., and A. Ghiorso, NNES-PPR 14B, 1604 (1949).

41. E. K. Hyde, M. H. Studier, and A. Ghiorso, NNES-PPR 14B, 1622 (1949).

42. D. W. Osborne, R. C. Thompson, and Q. Van Winkle, NNES-PPR 14B, 1397 (1949).

43. F. Asaro, Ph. D. Thesis, University of California Radiation Laboratory Unclassified Report UCRL-2180 (June, 1953).

44. J. M. Hollander, I. Perlman, and G. T. Seaborg, Revs. Modern Phys. 25, 469 (1953).

45. P. H. Stoker, M. Heerschap, and O. P. Hok, Physica 19, 433 (1953).

46. R. A. James, A. Ghiorso, and D. A. Orth, Phys. Rev. 85, 369 (1952).

47. J. E. Mack, Revs. Modern Phys. 22, 64 (1950).

48. G. L. Stukenbroeker and J. R. McNally, Jr., J. Opt. Soc. Am. 40, 336 (1950).

49. I. Perlman, P. R. O'Connor, and L. O. Morgan, NNES-PPR 14B, 1651 (1949).

50. F. Asaro, F. L. Reynolds, and I. Perlman, Phys. Rev. 87, 277 (1952).

51. F. Wagner, M. S. Freedman, D. W. Engelkemeir, and J. R. Huizenga, Phys. Rev. 89, 502 (1953).

52. F. Asaro, private communication (August, 1953).

53. J. K. Beling, J. O. Newton, and B. Rose, Phys. Rev. 87, 670 (1952).

54. G. T. Seaborg, R. A. James, and A. Ghiorso, NNES-PPR 14B, 1554 (1949).

55. G. T. Seaborg, R. A. James, and L. O. Morgan, NNES-PPR 14B, 1525 (1949).

56. W. M. Manning and L. B. Asprey, NNES-PPR 14B, 1595 (1949).

57. G. D. O'Kelley, G. W. Barton, Jr., W. W. T. Crane, and I. Perlman, Phys. Rev. 80, 293 (1950).

58. G. H. Higgins and S. G. Thompson, unpublished data (February, 1953).

59. H. Jaffe, private communication (July, 1953).

60. D. C. Dunlavey and G. T. Seaborg, Phys. Rev. (to be published, 1953).

61. E. Fermi, Z. Phys. 88, 161 (1934).

62. H. A. Bethe and R. F. Bacher, Revs. Modern Phys. 8, 82 (1936).

63. S. R. DeGroot and H. A. Tolhoek, Physica 16, 456 (1950).

64. G. Gamow and E. Teller, Phys. Rev. 49, 895 (1936).

65. R. E. Marshak, Phys. Rev. 61, 431 (1942).

66. J. C. Slater, Phys. Rev. 36, 57 (1930).

67. J. R. Reitz, "Relativistic Electron Wave Functions for a Thomas-Fermi-Dirac Statistical Atom," (Department of Physics, University of Chicago, 1949).

68. E. Feenberg and G. Trigg, Revs. Modern Phys. 22, 399 (1950).

69. M. G. Mayer, S. A. Moszkowski, and L. W. Nordheim, Revs. Modern Phys. 23, 315 (1951); L. W. Nordheim, Ibid., 23, 322 (1951).

70. M. E. Rose and J. L. Jackson, Phys. Rev. 76, 1540 (1949).